APPLICATION OF REMOTE SENSING IMAGES FOR ANALYSIS OF COASTLINE CHANGES

HARPREET KAUR A/P DALGIT SINGH

CIVIL ENGINEERING
UNIVERSITI TEKNOLOGI PETRONAS
JUNE 2010

CERTIFICATION OF APPROVAL

Application of Remote Sensing Images for Analysis of Coastline Changes

by

Harpreet Kaur A/P Dalgit Singh

A project dissertation submitted to the
Civil Engineering Programme
Universiti Teknologi PETRONAS
in partial fulfillment of the requirement for the
BACHELOR OF ENGINEERING (Hons)
(CIVIL ENGINEERING)

Approved by,

(Assoc. Prof. Dr. Saied Saiedi)

UNIVERSITI TEKNOLOGI PETRONAS

TRONOH, PERAK

June 2010

CERTIFICATION OF ORIGINALITY

This is to certify that I am responsible for the work submitted in this project, that the original work is my own except as specified in the references and acknowledgements, and that the original work contained herein have not been undertaken or done by unspecified sources or persons.

HARPREET KAUR A/P DALGIT SINGH

ABSTRACT

Coastline changes along 4 km stretch of Terengganu coastline, Peninsular Malaysia, has been detected by simple application of satellite images and the changes are related computationally to the environmental factors. The coastline stretch, near Sungai Besut, is formed by a fairly straight shoreline but is interrupted along 400 m by a river mouth. The area is protected by two breakwaters embracing the river mouth as well as by four groins to the north west of the river mouth. On the one hand, four high-resolution (2.5 m) satellite images were explored to detect the erosion or accretion rate along the shoreline. Hourly tide levels were taken into account to adjust the apparent waterline before the sediment volume of the coastline change was extracted from the overlaid images. On the other hand, the longshore sediment transport was estimated using empirical CERC formula. Comparison of the estimations from these two methods was made. It was shown that the analysis of the images backed by preliminary field data provides for a reliable detection of the past trends of coastline changes. The finding is promising in that the technique could project the changes into near-to-intermediate future as a safe estimation method for conceptual design purposes.

ACKNOWLEDGEMENTS

I would like to take the opportunity with deepest gratitude to thank Civil Engineering Department, Universiti Teknologi PETRONAS (UTP) for the FYP subject requirement to undergraduate level in this organization and for providing the equipments required to the completion of this study.

I would like to start by thanking my Supervisor, Assoc. Prof. Dr. Saied Saiedi, Senior Lecturer, Universiti Teknologi PETRONAS (UTP), first for the introduction of this topic. Although the beginning stage was tough for me, but I managed to get it all through, though there was a lot of struggle to complete the tasks. Thank you so much to indulge me so much into this topic and make me feel really comfortable with this topic now, not only for the thesis purpose but also future life interest. I would like to thank for your continuous support, advice and assistance. Your expertise, knowledge and practical experience in the coastal field was an amazing asset to have onboard and I have learned numerous practical skills from you. Thanks for pointing me in the right direction and keeping me in line. Your continuous support and guidance helped me throughout. Your amazing memory in coastal studies will never cease to amaze me.

I would like to thank Remote Sensing Agency Malaysia for their support and advice, besides providing all the remote sensing satellite images that has been used for this study, and also no charges applied for these images. Many thanks to Mr Syariman, Research Officer, Remote Sensing Data Services Section, for your professional insight in remote sensing analysis. I hope the results from this thesis will provide the necessary answers to some important questions in the future.

Special thanks to Coastal Engineering Department, Department of Irrigation and Drainage (DID) Malaysia, for allowing viewing all the previous reports for the study area at their library that helped for the input for this thesis. Thanks to representatives from DID, Mr Mohd Eizam and Miss Mashizam for their assistance with the reports and access to publications in DID Kuala Lumpur.

Thanks to Mr Jasmi, Senior Lecturer, Universiti Teknologi PETRONAS (UTP), and Mr Basith, PhD student at UTP, for spending time to introduce and get me familiar with Remote Sensing software, *ERDAS Imagine* and also encouraging me to learn the software into deeper extend. Although, not technically part of the department, you were the only people who knew this software, thanks for sitting in with me and teaching me the fundamentals of the image processing. However, I believe there is still a lot that I need to learn to get hold of this software comfortably.

Finally, I would like to thank my family, friends and classmates. Mum and dad, thanks for the constant support in many ways, I will forever be in debited to you. Thanks to my roommate who also supported me through all the emotional stress and break through. Thanks to all my friends who spent their time and helped me work out some tricky new methods, mates you all are just the best. Thank you for all your help and encouragement.

TABLE OF CONTENTS

LIST OF FIGURES

LIST OF TABLES

ABBREVIATIONS AND NOMENCLATURES

FYP	Final Year Project
UTP	Universiti Teknologi PETRONAS
GIS	Geographic Information System
NCES	National Coastal Erosion Study
DID	Department of Irrigation and Drainage
CERC	United States Army Coastal Engineering Research Center
AIRSAR	Airborne Synthetic Aperture Radar
TOPS	Total Operations Processing System
TOPSAR	Topographic Synthetic Aperture Radar
LANDSAT	Land-Use Satellite
MLLW	Mean Lower Low Water
MHW	Mean High Water
MOSTI	Ministry of Science, Technology & Innovation
ERDAS	Earth Resources Data Analysis System
RSO	Rectified Skew Orthomorphic
SPM	Shore Protection Manual
CEM	Coastal Engineering Manual
DEM	Digital Elevation Map
D_{50}	Mean grain size of sediment (mm)
d_b	Water depth at breaking point (m)
g	Gravitational acceleration (m/s/s)
H	Wave height (m)
H_b	Breaking wave height (m)
K	A dimensionless coefficient in CERC formula
K	Breaker index = H_b/d_b, usually close to 0.9
m	Beach slope normal to the shore (-)
n	Beach sediment porosity (≈0.4)
Q	Potential longshore sediment transport (m^3/s)
s	Relative density of sediment (≈2.65 for quartz)
α	Wave angle with the shore normal

CHAPTER 1

INTRODUCTION

1.1 Background of Study

Coastline, the boundary between land and sea keeps changing its shape and position continuously due to dynamic environmental conditions. Any long-term coastline change is a complex product of numerous actions of three major factors. (i) Environmental (wave, current, wind, river flow, sea-level changes). (ii) Human interference (coastal structures, dredging, coastal mining). (iii) Geology of coastal region. Engineering usage of satellite images (with a spatial resolution of a few tens of centimetres) and development of GIS techniques in the last three decades have become an invaluable supplement to the existing empirical and numerical tools to predict the long-term coastline changes.

Analysis of the past in coastline changes is often performed to predict the future changes. This analysis was traditionally based on field investigation aided by application of empirical formulae for wave transformation in the surf zone, longshore sediment transport, cross-shore sediment transport, and long-term beach evolution. Despite inherent complication of sediment motion in coastal waters, the predictive empirical equations have shown strong practical merits in estimation of short-term changes due to a series of storms (USACE, 2010) and (SATO S, 2000).

Detection and measurement of shoreline changes are an important task in environmental monitoring and coastal zone management. There are many ways to detect the shoreline changes. One way is the multispectral remote sensing satellites providing digital imageries in infrared spectral bands. Satellite optical images are simple to interpret and easily obtainable. Absorption of infrared wavelength region by water and its strong reflectance make the images an ideal combination for mapping the spatial distribution of land and water was pointed by De Witt (2002). Coastline changes are usually expressed in linear terms, as the extent of advance or retreat measured at right angles to the land margin, but they can also be considered in aerial terms, as the extent of land gained or lost on a coastal sector, or volumetric terms, as the quantity of material added to it, or lost from, the coast.

1.2 Problem Statement

Malaysia is situated in the Southeast Asia, between Latitudes 1° and 7° north, and Longitudes 100° and 119° east. It comprises of two regions, Peninsular Malaysia and the states of Sarawak and Sabah on the northern part of the Borneo Island. The surface area is about 330, 400 km². These regions are separated by 640 km of South China Sea. Malaysia's coastline is over 4, 809 km where more than 1, 300 km of Malaysia's beaches are experiencing erosion (NCES, 1985). This has since increased to 2, 327 km that it means from 47 sites to 74 sites in 2000. **Figure 1.1** shows the Malaysian coastline.

Figure 1.1: Malaysia Coastline

This 4, 800 km of coastline comprising of two distinctly different physical formations namely the mangrove fringed mud flats and sandy beaches. The Eastern coast of Peninsular Malaysia consists of straight sandy formations in the North and a series of hook or spiral shaped bays to the South. The Western coast of Peninsular Malaysia comprises mainly muddy formations, with limited areas of pocket sandy beaches. In Sarawak and Sabah, the coastline is about equally divided between sandy beaches and mud coast. **Figure 1.2** shows the classification of the coastal sediments in Malaysia.

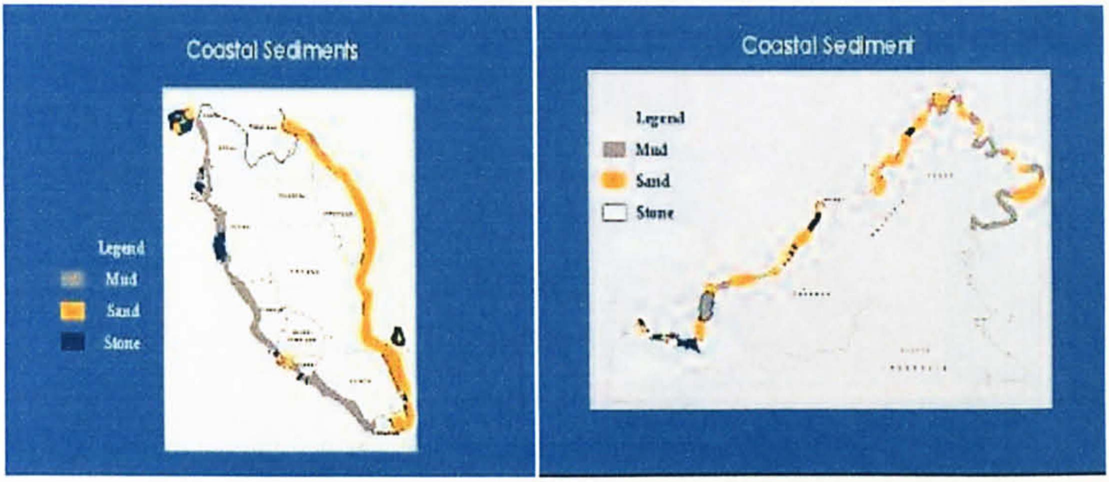

Figure 1.2: Coastal Sediments in Malaysia

Erosion occurs due to natural causes and interference of nature by man. Along the coast, the sediment is continuously being moved. When the rate of sediment entering and leaving the coast equals, the coast is said to be in dynamic equilibrium (Abdullah, 1993). Erosion occurs when, over a period of time, the volume of sediment transported out is greater than that transported into the coast. From November 1984 to January 1986, the Government carried out the NCES to study the increasing incidences of coastal erosion, and the study results indicated that out of the country's coastline of 4, 809 km, about 29% or 1,380 km was facing erosion. This study distribution was determined through the NCES 1985 and updated recently by Coastal Engineering Division, DID Malaysia in May 2005 (NCES, 1985). Erosion may be amplified during monsoon period when high water levels, associated with the reason, result in waves breaking directly against the scarp, causing loss of material. Though some of this material might be returned to the shore by the swells after the monsoon, the quality returned is normally much less; hence the net result is erosion. Based on NCES 1985, Malaysia's coastline are classified into three categories of erosion and the threat to existing shore based facilities of substantial economic value and defined as follows (DID Malaysia, 2008):

i. **Category 1**: Shorelines currently in a state of erosion and where shore- based facilities or infrastructure are in immediate danger collapse or damage; this includes 140 km of Malaysian coastline.
ii. **Category 2**: Shoreline eroding at a rate whereby public property and agriculture land of value will become threatened within 5 to 10 years unless remedial immediate action is taken; 240 km of Malaysian coastline is in this category.
iii. **Category 3**: Undeveloped shoreline experiencing erosion but with no or minor consequent economic loss if left unchecked; this involves 900 km of Malaysian coastline.

The list of coastal erosion areas in Malaysia is showed in **Appendix 1**. Amongst the total coastline, 62.5% of Terengganu, approximately 152.4 km is eroding (DID Malaysia, 2008). The study has clearly pointed out that a primary cause of coastal erosion is poor citing, planning and design of coastal development projects and activities. Hence in addition to implement long term strategies emphasizing on proper planning, regulation and control of future developments in the coastal zones. **Appendix 2** shows the summary of eroding coastline in Malaysia for Peninsular, Sabah and Sarawak.

1.3 Objectives of Study

The study presents an application of remote sensing images to estimate long-term coastline changes caused by coastal structures built at the river mouth of Sungai Besut in Terengganu, Malaysia. The objective of this study is to put forward a simple procedure to use x-y satellite images for analysis of long-term coastline changes. To identify and quantify historical shoreline change and the processes that induced changes. The method is based on correction of the shoreline position to incorporate the impact of tide, overlaying of successive images, and volume estimation from a local knowledge of the average beach slope. The procedure is applied to a case in Malaysia and the finding is substantiated by longshore transport estimation based on the well known CERC formula (USACE, 2010). And to identify any trend in terms of dynamics of the sediment budget around the river mouths of the various estuaries along the coastline and finally able to predict the future coastline changes.

1.4 Scope of Study

This study focuses on the East Coast Peninsular Malaysia, shoreline Kuala Besut Terengganu. Terengganu has a sandy coastline of 244 km. Based on NCES (1985), Malaysia's coastline is classified into reaches, and Kelantan is in Reach 2E and Kuala Besut in Subreach 2E1. This subreach is approximately 18 kilometers long and extends from Pengkalan Datu River southeast to Kampung Kuala Besut. Refer to **Appendix 3** showing the Coastal Reaches of Peninsular Malaysia.

Figure 1.3 shows the study area in the East Coast of Peninsular Malaysia facing the South China Sea. It is located between latitudes 102° 32' 04 92" and 102° 32' 05 88" East, and longitudes 5° 49' 02 42" and 5° 50' 48 66" North. The shoreline is 4 km and is interrupted by a river, locally called Sungai Besut (Sg. Besut). The climate is characterized by Northeast Monsoon prevailing between November and March. Annual average temperature is 25.6°C~27.8°C and the tide are of diurnal type with a range between 1 to 2 m. The wave window exposure at the site is from 180°N to 330°N with wave height less than 1.8 m (Rosnan *et. al*, 1995) and (Lokman *et. al*, 1995). With a catchment area of 1,230 km^2, Sg. Besut originates from the Main Range of Peninsular Malaysia and drains into the South China Sea with its mouth situated on the east coast of Terengganu State, immediately south of the Kelantan and Terengganu border.

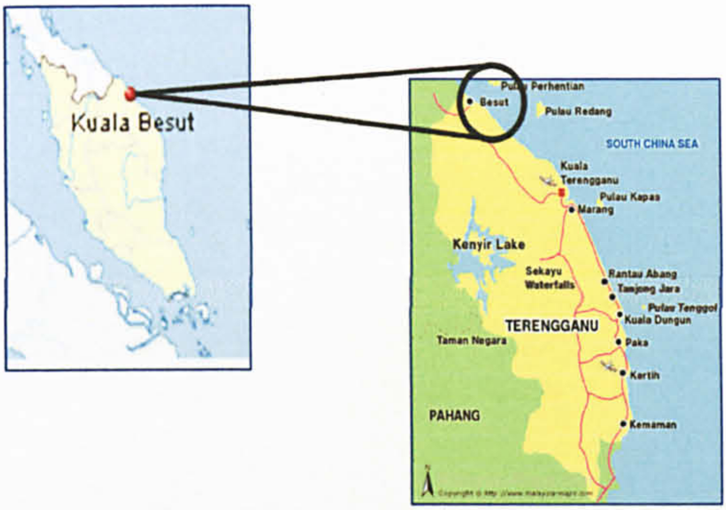

Figure 1.3: Location Map of the Study Area, Sungai Besut, Terengganu Coastline

The river has an annual average flow of 20~70 m^3/s, an annual maximum flood of 350~1000 m^3/s, and an annual minimum flow as low as 5 m^3/s. Based on a recent consultancy study on the improvement of the river mouth AIS Consultants (2009), Kumarasivam Tan & Ariffin Sdn, Bhd. (1987) and Kumarasivam Tan & Ariffin Sdn, Bhd. (July 1988), the maximum flood tide and ebb discharges were found to be 173 m^3/s and 220 m^3/s, respectively. The river is estimated to bring annually 100,000 m^3 of sediment. The river bed material is predominantly coarse sand with mean particle size, D_{50}, of 1~2 mm. The river has a bed gradient of about 1:4000 and velocity of about 2 m/s during flood flows. From 1963 to 2005, the downstream reach of the river has been dredges at least three times to maintain a minimum navigability for local fishers.

To protect the river mouth against large sedimentation from the river, longshore sediment transport, and serious wave attack, two breakwaters were constructed in April 1998, followed by four groins constructed in 2004 to protect the west coast against serious erosion in the updrift part of the coast (**Figure 1.4**). The shorter breakwater is **205 m long with 40° with north and the longer one is 305 m with 140° with north. The** groins are 60 m long with spacing of 120, 125 and 105 m. The river mouth is 400 m wide and breaks the study reach into two beaches, each 1.8 km long: west beach that includes groins and east beach that ends at the longer breakwater.

Figure 1.4: Rivermouth and the Existing Structures (2 Aug 2005)

Figure 1.5 shows the groin at Kuala Besut. **Figure 1.6** and **Figure 1.7** shows the left and the right breakwater at Kuala Besut. **Figure 1.8** shows the breakwater at Kuala Besut.

Figure 1.5: Location photo at groin of Kuala Besut

Figure 1.6: Location photo to the left of Kuala Besut left breakwater

Figure 1.7: Location photo to the right of Kuala Besut right breakwater

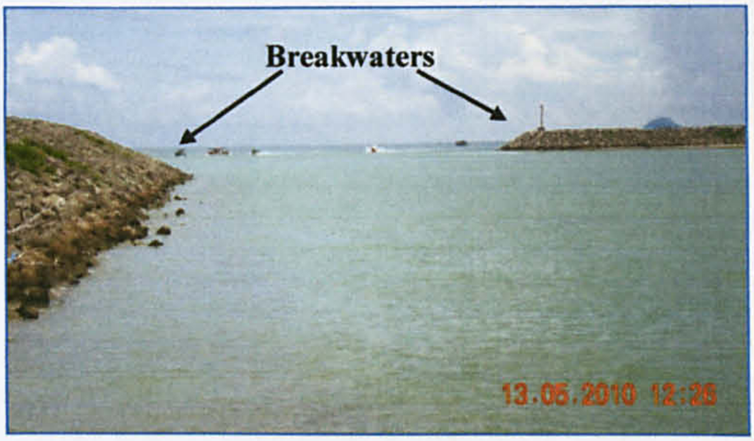

Figure 1.8: Breakwaters at Kuala Besut

The south breakwater in particular will block the littoral transport and lead to coastal impacts. The pre breakwaters' era, the sedimentation problem has been mainly due to the littoral drift. The breakwaters have prevented the drift and resulted in sand accumulation on the up drift and erosion on the down drift area. The breakwater with entrance width of 120m was completed in April 1998. The construction of the breakwaters has resulted in sand accumulation on the up drift side of the structures as well as erosion on the down drift area. Since the long shore transport has been blocked by the breakwaters, the sedimentation within the river mouth has been mainly due to the riverine sand source. The heavy sedimentation rate at the river mouth is due to the high sediment load from the river discharge. The rate of erosion on the up drift section is relatively high and among the mitigation measures was the introduction of groins. However due to high erosion rate, the groin has been ineffective.

A classic coastline study report in Malaysia (NCES, 1985) classifies the beaches of Terengganu as having '*acceptable erosion*'. According to the annual report of the Department of Drainage and Irrigation in 2007, 62.5% of all 244 km beaches in Terengganu have noticeable erosion, including 20 km of '*critical*', 10 km of '*significant*' and 122.4 km of '*acceptable*' erosion. AIS Consultants (2009) presents study area as an example of significant net erosion.

Figure 1.9 presents satellite views of the study area in successive: **Figure 1.9 a** shows the overall view of the 4-km-strech that includes 400-m-river mouth and two 1.8-km-beaches at each side, west and east. **Figure 1.9 b** presents a close view of the river mouth and the breakwaters. **Figure 1.9 c** shows the west part of the coastline that includes a series of four groins. **Figure 1.9 d** contains views of the east part ending at the longer breakwater. The overall evolution of the coastline at various places is clearly seen in these figures: net deposition along the east beach and erosion along the west beach.

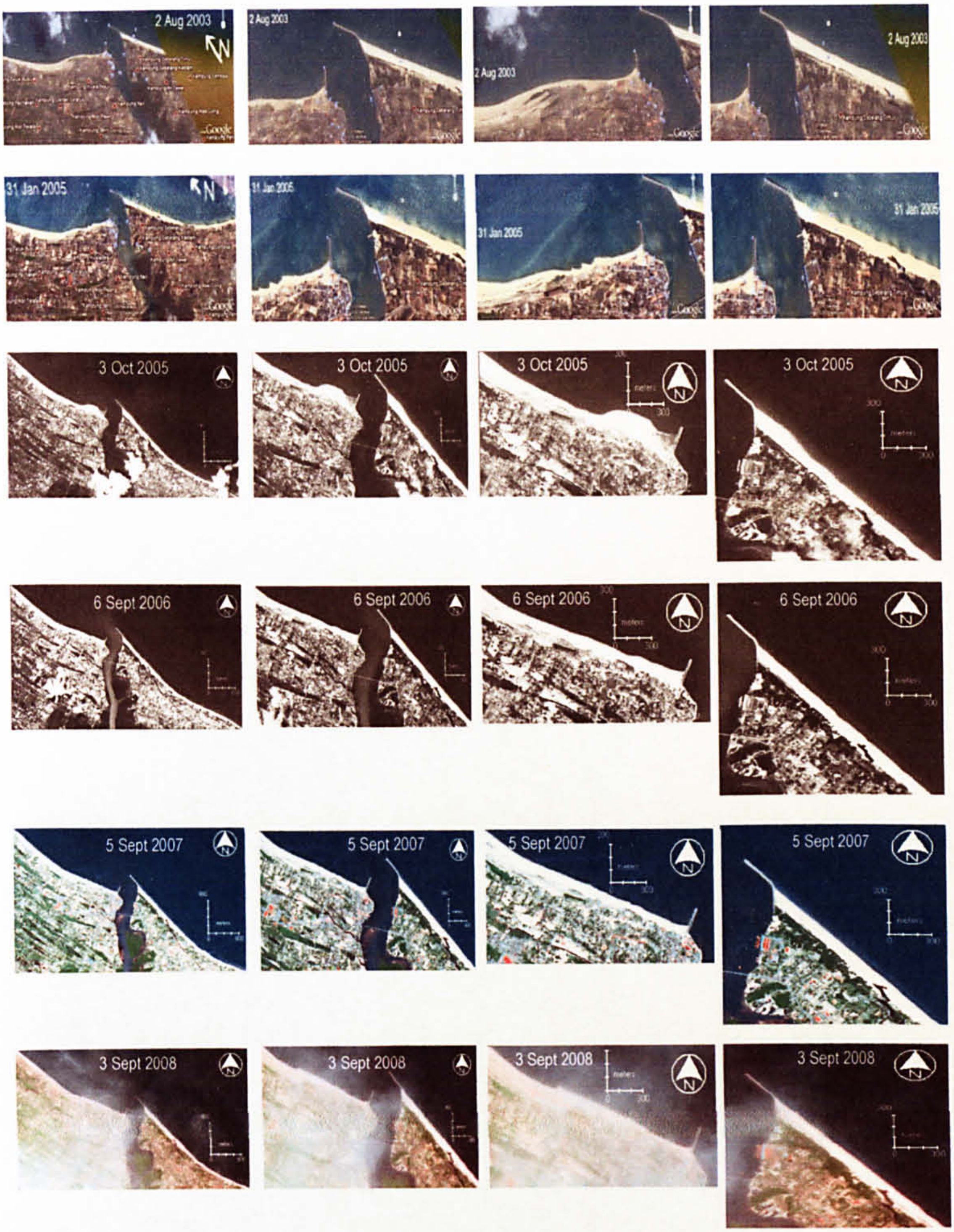

a. Overall view

b. Close up of the river mouth and the breakwaters

c. West part of the river mouth (including groins)

d. East part of the river mouth

Figure 1.9: Various Views of the Study Area, Sungai Besut, Terengganu Coastline

CHAPTER 2

LITERATURE REVIEW

2.1 Coastal Erosion

Coastal shorelines worldwide are changing rapidly as a result of natural physical processes and whereas human activities are catalysts causing disequilibrium conditions that accelerate changes (Saied Choopani, 2000). The natural processes include phenomena such as waves, currents, and storms. Examples of human activities affecting the shoreline and land reclamation, recreation at beaches, land use practices and construction in coastal zones. Coastline changes produce a positive or negative impact. For instance, coastline accretion may create more usable land for recreation for other purposes, which is a positive phenomenon. Changes in the shape of the coastline may fundamentally affect the environment of the coastal zone. Coastline monitoring is an important step in many coastal engineering projects such as harbor construction and for coastal protection. Furthermore, coastline change detection is an important environmental parameter, i.e. in connection with erosion from storm impact or human disturbance.

Coastal erosion is defined as the gradual wearing away of the Earth's surface by the action of natural forces of wind and water (Rongxing Li, 2000). Coastal erosion is a natural process. Control of coastal erosion has now become an important economic and social need. The coastal features susceptible to change through external forcing usually represent the integrated responsible, the shore zone to a number of interacting environmental variables operating across a broad spectrum of time scale. Whereas the interactive forces and geological and hydrodynamics processes and climate condition causes changes of coastline situation and create transgression and regression coastlines.

Advance or retreat of a coastline may result from combinations of erosion and deposition, emergence and submergence. Coastline changes can be mapped and measured on various coastal sectors over time scales ranging from a few hours or days to long- term trends over decades or centuries. Evidence of changes can be obtained from comparisons of dated historical maps, charts, air photographs, and satellite imagery with the present coastal configuration. Such evidence is available on many coasts over the past century, but the analysis methods that differ always make an impact on the study and the results obtained.

The investigation of changes in coastline position or morphology can aid in predicting the life expectancy of coastal infrastructure, but may also point to more complex trends in coastal stability, sediment supply, and crustal movement. It may be difficult to isolate the particular cause of a change is coastal position, morphology, or other properties; or a change in the rate, frequency, or intensity of coastal processes (Saied Choopani, 2000). The shoreline change detection and mapping are critical for safe navigation, coastal resource management, coastal environmental protection and sustainable coastal development and planning (B. Shaw, 1995).

2.2 Detection and Measurement of Shoreline Changes

Studies done previously on the study of the coastline long term changes has adapted many different ways to interpret the images obtained and also applying different software to analyze the images. The rates of the shoreline position changes are frequently employed to summarize historical shoreline movements and to predict the future shoreline. The data used to calculate a rate of shoreline changes consist of a number of shoreline positions within a time period. Shoreline position data sources may include historical maps and aerial and satellite photographs. Each shoreline point possesses a degree of uncertainty that may arise from; for example, the difficulty of precisely timing the water surface level (e.g. mean high water) and other error sources (Saied Choopani, 2000).

Remote sensing images are used to classify the changes of coastline in different periods. (J.Y., 1998) and (Li X., 1998) performed many successful studies to monitor shoreline changes by using multi- temporal satellite images and the precision of this method depends on the spatial and spectral resolutions of remote sensing data that is limited because of the data resources. The other aspect depends on the correctness of registering and matching multi – temporal remote sensing images, which is the most important factor and will influence greatly the result of whole research, as it is the basis of following processes. The accuracy of classified results, which is the key point in the method, and will determine later the accuracy if area statistics for growth lands caused by changes of coastlines. Zhu (2001) presented the precision of image geometric correction and the accuracy of digital coastline vectors.

Coastline changes can be mapped and measured on various coastal sectors over time scales ranging from a few hours or days to long- term trends over decades or centuries. Evidence of changes can be obtained from comparisons of dated historical maps, charts, air photographs, and satellite imagery with the present coastal configuration. Such evidence is available on many coasts over the past century, but the analysis methods that differ always make an impact on the study and the results obtained.

Nowadays the usage of satellite images and the application of GIS techniques have been so popular since it is able to supplement to the existing empirical and numerical tools to predict the long-term coastline changes. Satellite images are simple to interpret and easily available from the government agencies for study purposes. Absorption of infrared wavelength region by water and its strong reflectance make the images an ideal combination for mapping the spatial distribution of land and water (DeWitt, 2002).

There are also studies to monitor environmental changes using a difference approach for the images taken of same geographical location but at different times. This is by doing orientation of images; the differences between consecutive data sets displayed on one picture will immediately reveal environmental changes that happened in the time between. This approach, called the photogrammetry obtain results that are far more precise and clear enough to confirm the introduced method, and this method is an effective approach to monitor coastal land use status for large area (Karsli, 2003). In this study, the aerial photographs were obtained in two different times. By examining the photographs, it is apparent that coastal zone of the study area has been changed drastically in the course of time. The digital photogrammetric approach utilizes digital images to do all the measuring and digitizing works. In this respect, high-quality digital images are required for use in digital photogrammetric processing. Besides, the processes of duplicating film and scanning positives should be done required geometric resolution with extra caution.

Through the object oriented technique, the images objects were also imported into ARCGIS environment and vector base coastlines can be produces, for the purpose of calculating the changes during the time period which is considered. Coastal erosion studies by using time series analysis of map sheets and IRS-L1 satellite data (Ghosh, 1995). It can be said that using aerial photo alone for shoreline change considers as unperfected study to investigate the problem of erosion and sedimentation. The integration between other type of remote sensing data and coastal processes model is more optimize to investigate shoreline change for large scale. This can be drawing a wide view on shoreline change pattern.

AIRSAR/TOPS data was utilized by Maged Marphany (1998) to detect shoreline change along Terengganu coastline. TOPSTAR data was used to extract information on wave spectra. This wave spectra information was then used to model shoreline changes by investigating the wave refraction patterns. From these patterns, the volume transports at several locations were estimated. The shoreline change model developed was designed to cover 20 km stretch or shoreline of Kuala Terengganu. The model utilized date from aerial photo, TOPSAR data and ground truth data. The location of sedimentation and erosion along shoreline of Kuala Terengganu was estimated. A comparison between TOPSTAR shoreline change model and aerial photo and ground truth data showed a significant relationship.

Different historical data of satellite imageries, aerial photo and topographic maps is also used to detect shoreline change by Raj (1982), Mazlan (1989) and Frihy O.E. (1995). Most of these studies found an impossible rate of erosion occurred. For example Frihy O.E. (1995) found there is a significant relation between shoreline changes estimated form the LANDSAT and aerial photo and ground survey.

Morang *et. al* (1997), Larson *et. al* (1997), Morang *et. al* (1997) and Gorman *et. al* (1998) in a series of articles outlined the principles of monitoring the coastal environment with some reference to aerial photography. Li *et. al.* (2001) presented a method to compute the instantaneous shoreline and to derive Mean Lower Low Water (MLLW) and Mean High Water (MHW). Hennecke (2004) applied GIS to model sea-level rise induced shoreline changes inside coastal re-entrants of two Australian regions. An application of remote sensing technology for coastal studies in Malaysia has gained momentum in the current decade. Chalabi *et. al* in 2004 and 2006 employed IKONOS images and aerial photographs to monitor the coastline changes near Kuala Terengganu. In 2006, Zakariya *et. al* used *Landsat-5* and *Landsat-7* images to detect changes in the river mouth of Terengganu River. Ibrahim in 2009 used public domain images available on *Google Earth* to supplement a preliminary site analysis of coastline erosion in north Terengganu regions.

CHAPTER 3

METHODOLOGY

3.1 Data Collection

From the beginning of the study, the important consideration to understand the project is done with serious literature review to grasp overview of the project and on the different methods used for the analysis of coastline changes as has been discussed earlier. This was done through research into journals and conference papers on the internet and also resources in the library. Besides that, studies on relevant books to understand the big picture of this study.

Many reports were viewed from the Department of Irrigation and Drainage (DID). Following are the supporting materials obtained from DID that were reviewed to better understand the subject matter:

1. National Coastal Erosion Study 1985 Volume 1 & 2
2. Investigation on Rehabilitation Works in Sungai Besut Coast in Terengganu, 2009
3. Besut Flood Mitigation Project, Final Project, Volume 1: Main Report, 1987
4. Besut Flood Mitigation Project, Final Report, Volume 2; Supporting Appendices to Main Report, July 1988

Through thorough literature review and based on the availability of the resources, remote sensing images were requested from the Remote Sensing Agency, Ministry of Science, Technology & Innovation (MOSTI). Data available for this study involves four different dates for different years. Remote sensing images of Satellite Sensor SPOT- 5 with 2.5m resolutions on the study area, dated 3rd October 2005, 6th September 2006, 5th September 2007 and 3rd September 2008 were analyzed for this study.

This study plays emphasis on the output by change detection method (overlaying) of the location SPOT-5 images, for the four different years to detect the pattern change at the study location. The images were operated in *ERDAS Imagine® V9.1. ERDAS Imagine* is the raster- centric software GIS professionals use to extract information from satellite and aerial images. *ERDAS Imagine* is easy-to-use, raster-based software designed specifically to extract information from images. With its vast array of tools, it allows analyzing data from virtually any source and presents it in formats ranging from printed maps to 3D models; *ERDAS Imagine* offers a comprehensive toolbox for all of the geographic imaging and image processing needs. With three tiers and a multitude of add-on modules, it enables building exactly the system needed.

3.2 Image Processing

Analysis of coastline changes involves the different satellite images that can be used to supplement the analysis. In this study, the remote sensing SPOT-5 satellite images are used to perform the change detection analysis (overlaying). The SPOT-5 images possess high resolution outputs of 2.5m resolutions. What this means is that the images are clear for any objects larger than 2.5m on ground. For the case of coastline changes study, these images prove to be good. To analyze the remote sensing images, it was operated in *ERDAS Imagine*, a comprehensive and sophisticated tool for digital analysis of remotely sensed data. To be able to reach to the final output for the change detection analysis, some other functions are fulfilled.

The **image re-projection** process is transforming, three-dimensional space onto a two dimensional map. This process inevitably distorts at least one of the following properties: shape, area, distance, direction, and others. Theoretically map projection might be defined as "a systematic drawing of parallels of latitude and meridians of longitudes on a plane surface for the whole earth or a part of it on a certain scale so that any point on the earth surface may correspond to than on the drawing".

An ordinary globe is rendered useless for reference to a small country. It is not possible to make a globe on a very large scale. Moreover it is neither easy to compare different regions over the globe in detail, nor convenient to measure distances over it. Therefore for different types of maps different projections have been evolved in accordance with the scale and purpose of the map.

There is no ideal map projection, but representation for a given purpose can be achieved. The selection of projection is made on the basis of the location and the extension of the feature of the globe. This includes the shape of the boundary to be projected and the deformations or distortions of a map to be minimized.

For the Malaysian Datum (East Malaysia), adopts the Modified Everest ellipsoid as a reference with its origin fixed at Kertau, Pahang. The existing coordinate systems used for mapping and cadastral survey in East Malaysia are the conformal Rectified Skew Orthomorphic system (RSO). The RSO projection system is also based on the Modified Everest. **Figure 3.1** gives an idea of the image re-projection through Montage Re-Projection Model.

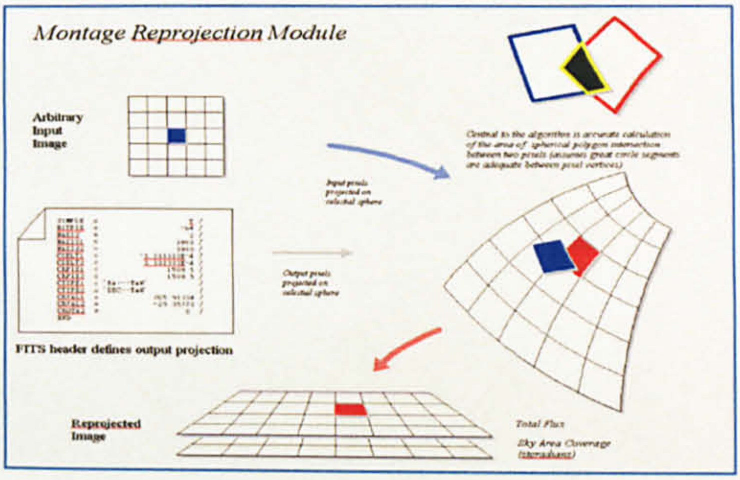

Figure 3.1: Image Re-projection

Images acquired at different times usually have different amounts of haze, dust and clouds in the atmosphere. These differences can mask real changes or make similar land cover appears to have changed. Before comparing the differences between the images, it is important to make sure that the images can properly align to each other. This is referred to as **image rectification.** If the case of this study, the images actually align to the real world coordinates, so these images will also be geo-referenced. Since the images for this study were not aligned properly, so the rectification was done before a change detection analysis or the detail comparison can be done. **Figure 3.2** shows the view during performing rectification in *ERDAS Imagine.*

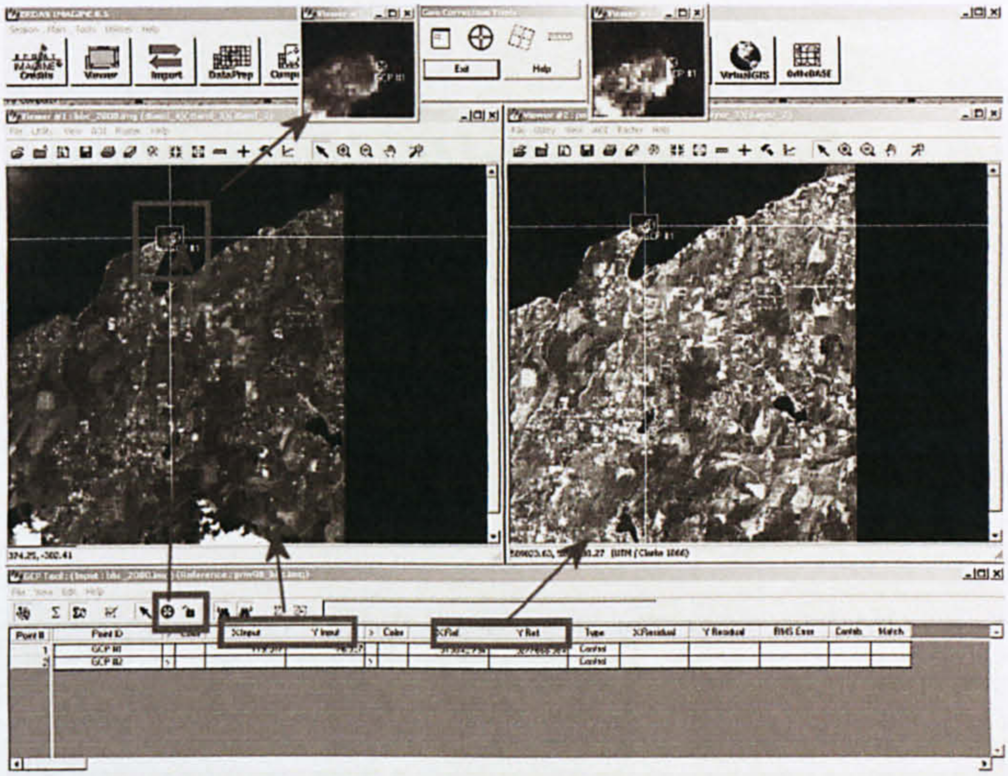

Figure 3.2: Image Rectification in *ERDAS Imagine*

The first method to check alignment is to visually inspect the images. Two (or more) windows are opened in *ERDAS Imagine* and load an image in each. Resize the windows so they are large enough to show detail and can fit side by side on the screen at the same time. Make them the same size by temporarily overlaying one window on the other and dragging a corner to align them. Rearrange the windows for easy viewing and geo- link them. Then, zoom into various features within the scenes to compare the two images. The important note is to check the alignment at multiple locations around the scenes.

After the images are properly rectified, and before performing any other preprocessing, spatial **sub-setting** is done on the images to reduce the area of analysis. Typically it is simply sub-setting an image by cutting a rectangular area around the region of interest. Basically, the image is zoomed in to an area slightly larger than the study area, adjusting the window height and width to interest. The images can be cut using the image cell coordinates as preferred. Cutting the first image is the easy part. Sub-setting a second image, to exactly the same footprint as the first image, can be done by input of the same coordinates as the early one. The new subset image will resize the aspect (height and width) of the window to fit the entire dataset. The result are two images of the same size (within a fraction of a pixel) covering the same area of interest. **Figure 3.3** gives an example of subset image output from *ERDAS Imagine.*

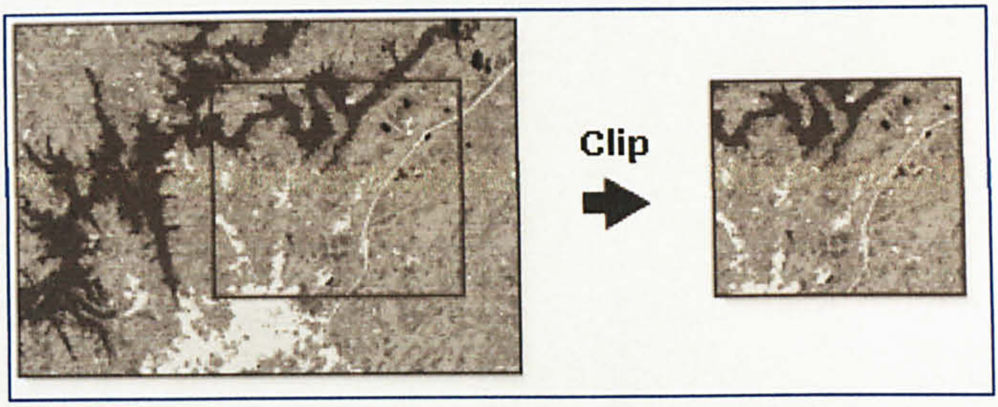

Figure 3.3: Image subset in *ERDAS Imagine*

Remote sensing data is now popular for the application for change detection. In order to monitor the coastline changes along the study area, a change detection analysis (overlaying) was performed to determine the movement of the coastline through years. **Change detection** is a technique used to determine the change detection between two or more time periods of a particular object of study. Change detection is an important process in monitoring and managing the coastline changes and it also provides quantitative analysis of the area changes over the years. The aim of change detection is to find pixels in pairs of co-registered images that correspond to the real changes on the ground. Change detection is the process of identifying differences in the state of an object or phenomenon by observing it at different times according to (Singh, 1989). Prior to any change detection, it is imperative that the imaginary be geometrically rectified so that the pixel at one date overlaps the same pixel for the other date (Townshnd *et.al.*, 1992).

The advantage to perform the change detection in *ERDAS Imagine*, that it also allows to compute affected area due to the changes within the software. The area computed will be used to analyze the images and also conclude the coastline changes in this study.

3.3 Engineering Calculation

3.3.1 Basic Field Data

Site assessment was done to obtain sediment samples to conduct sieve analysis and to do land surveying to measure the beach slope. During the site assessment, two representatives from the DID Besut were along to familiarize on the site and also the activities that have taken place for the past years near the study area.

Sediment samples collected during the site assessment were collected and labeled accordingly. **Figure 3.4** showing the sample collection at site. **Appendix 4** shows the locations where the samples were taken and the sample labeling. Sieve analysis is done for the sample collected at various locations at Kuala Besut beach and results for the sieve were noted and the grain size distribution is plotted in log graph in EXCEL spreadsheet. The sieve analysis results for each sediment samples in tabular and graphical order are presented in **Appendix 5**. **Figure 3.5** shows during conducting sieve analysis in the lab.

Figure 3.4: Collecting sample at site

Figure 3.5: Conducting Sieve Analysis

This sieve analysis will provide some understanding on the beach material distribution along the coastline. The average value for sand grain mean diameter (D_{50}) which showed the size of sediment with 50% finer is obtained from the sieve graph. The summary of mean diameter (D_{50}) of sediment size distribution for each sample is shown in **Table 3.1.**

Based on the different values obtained for mean diameter (D_{50}) of sediment size distribution for the samples, D_{50} adopted for this study is 0.36mm.

Table 3.1: Summary of mean diameter (D_{50}) of sediment

Sample Labels	Sediment Mean Diameter, D_{50} (mm)
1	0.43
1A	0.25
1B	1.00
2	0.57
2A	0.36
2B	0.45
3	0.31
3A	0.59
4	0.27
4A	0.27
4B	1.45
5	0.37
5A	0.24
5B	1.5
6	0.31
6A	0.13
6B	0.28

Slope measurement on the site was done using the total station. Slope of the beach is very important for the tide correction for this study. With the details on the beach slope for the coast, the difference in the high tide and the low tide and the calculation, the values of the differences of the high tide line and low tide line from the normal coast line can be estimated. This would give the area of land affected and assist for the images analysis. **Figure 3.6** shows during slope measurement using total station.

Figure 3.6: Slope measurement using the total station

Slope measurement was only done for the area behind the right breakwater during the site assessment. Data extracted from the total station was analyzed on *AUTOCAD Land Development*. Based on that output, data was analyzed and measurements for the slopes at different locations are presented in **Appendix 6**. Based on the results for the slope, there is wide range of slopes for the different locations at the beach. The average beach slope as calculated is found to be 1:15 to 1:20. However, the slope value used in this study calculation is taken to be 1:40. The summary of beach slopes for the each location is shown in **Table 3.2.**

Table 3.2: Summary of beach slopes

Slope Location	Slope	
	Readings	Approximate Slope
1	1.889 : 70.402	1:37
2	1.758 : 35.074	1:20
3	1.585 : 34.764	1:22
4	1.647 : 33.115	1:20
5	2.035 : 35.44	1:17
6	1.983 : 50.587	1:26

The Northeast Monsoon, which starts in November and December and usually lasts until March affect the East coast of Peninsular Malaysia. The east coast of Peninsular of Malaysia is not significantly affected. Wave rose representing the percentage (%) frequency of occurrence of deepwater wave heights and deepwater wave approach directions for 35 years of observations (1949-1983) is analyzed and discussed in the next section. Wave heights on the east coast of Peninsular Malaysia during the Northeast Monsoon period are generally less than 1.8 meters with a period of less than 6 seconds, but can vary greatly due to the alternating periods of strong winds and calm. Wave rose is interpreted to consider the effects of wave onto the beach for the study area.

3.3.2 Tide-correction of the shoreline

Tide plays a big role on the interpretation of the satellite images. Tidal information is necessary to determine the local wave regime. The tidal heights are obtained from the Royal Malaysian Navy Tide Tables and the Malaysian Survey and Mapping Department Tide Tables. The nearest Standard Port to the study area is the Kuala Terengganu station at Latitude 05 21 N and Longitude 103 08 E. These images obtained from the Remote Sensing Agency are captured at 11.00 am, so this marks the time of interest. Based on the information on the timing of the images at 11.00am, the tide height at the time is marked. **Figure 3.8 (A&B)** shows the beach observations during high tide and low tide for the one particular day. From here, it can be observed that during high tide, more shore area is covered with water and the waterline is moved to the land and during the low tide, more beach area is exposed and the waterline is moved to the sea. This can influence the estimation of the shoreline if comparisons of the coastlines are merely done straight from these images. The tidal consideration would give a meaningful effect for the interpretation of the area eroded or deposited on the images.

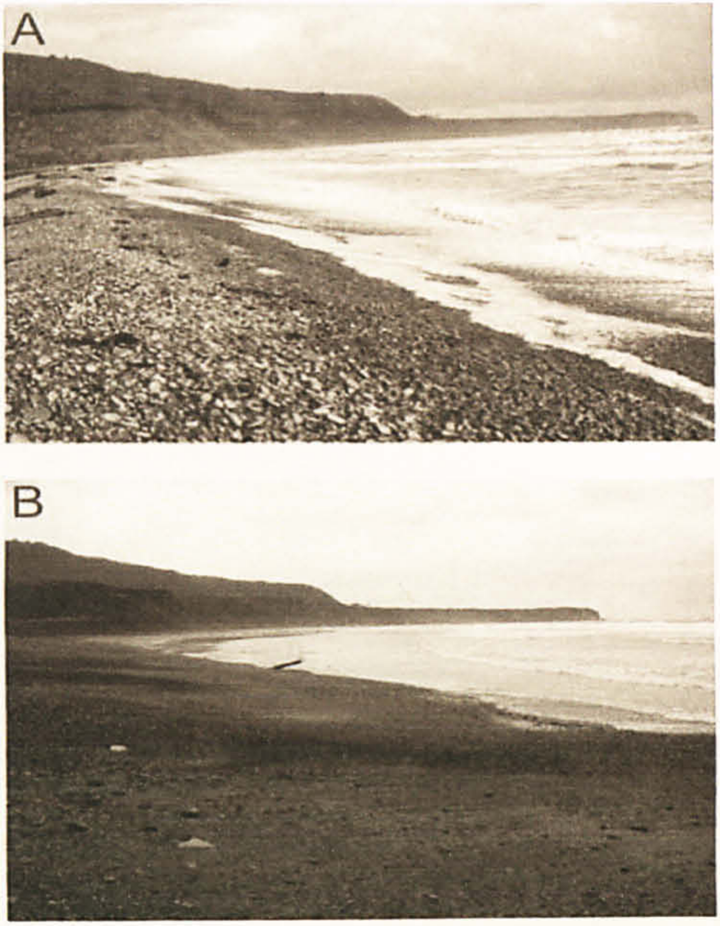

Figure 3.8 (A): Beach during High Tide
(B): Beach during Low Tide

3.3.3 Estimation of sediment transport

In this study, the consideration of the longshore sediment transport and its affect on shoreline change has been investigated and discussed. It is clear that the along-shore sediment transport rate is an important parameter for shoreline change estimation. The procedure to mathematically predict the volume of transported sediment in the coastal areas requires knowledge of the magnitude and direction of the energy flux due to waves breaking along the coast of the area where the study is performed. U.S. Army Corps of Engineers, (USACE, 2010) in their publication proposes to quantity the along-shore transported sediment, a wave climate representative of the annual wave conditions measured or experienced in offshore waters must be established. The wave climate is in the form of a set of wave heights with different periods and directions, which must be "routed" towards shore by a wave refraction model until the waves break on or near the beach. Information on their breaking angles relative to the beach orientation, breaking wave heights, and wave speed at breaking should be determined and used to establish the along-shore components of the energy flux for the two directions along the shore. To establish a representative wave climate, proper understanding of the directional distribution of wave height and wave period is needed, since the distribution of wave heights is converted to an equivalent distribution of wave energy that is a function of the along-shore sediment transportation rate.

3.4 Comparison and Interpretation

Based on the results obtained from the areas computed result of the change detection analysis (overlaying) and also results from the longshore sediment transport from CERC; comparison is done to the values of total net annual transport and the change in beach width is done. However, there are many limitations to the study due to insufficient data available. Based on the images available and also comparing to the site assessment, comparison of the past and present is also discussed.

CHAPTER 4

RESULTS AND DISCUSSION

4.1 Image Processing

The image in **Figure 4.1** shows the *unsupervised classification* analysis of the image processed in GIS software (*ERDAS Imagine*).

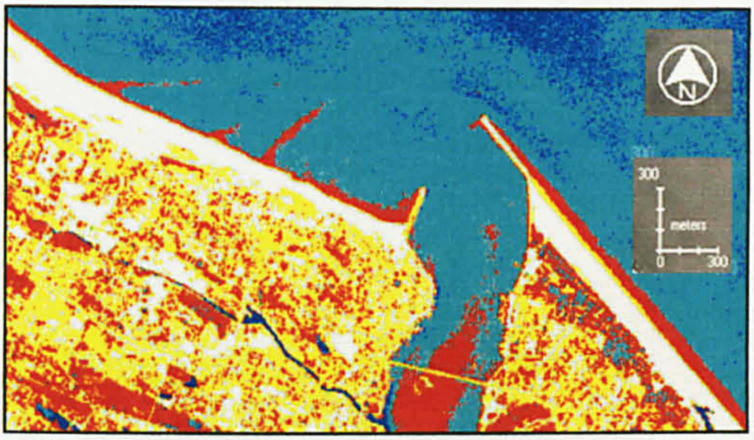

Figure 4.1: Unsupervised Classification Image of the Study area processed in *ERDAS Imagine*

Unsupervised classification is used to cluster pixels in a data set based on statistics only, without any user-defined training classes. This method does not require user to input details to create the classified image and the output tends to require a great deal of post classification operations to make the results more meaningful. With an input of five classes, the image develops different colours for sedimentation, sea, land area, vegetation, and deep sea. The interpretation of this image shows heavy sedimentation in red (darker regions in the B/W print) in the middle of the river outlet (a large sandbar), along the east coast, and near groins. These features cannot be seen in the raw images.

4.2 Tide Level Correction and Image Overlaying

This study incorporates the importance in tide levels to determine the position of beach waterline when the different satellite images are compared. The fact that tide level determines the position of beach waterline should be taken into account when different images are compared. A level difference of 2 m at a beach with a typical beach slope of 1:50 results in 100 m shift in the waterline. To omit the consideration of the tide effects onto the affected beach width would give a complete misinterpretation of the coastline changes. The waterline in *unprocessed images* (such as aerial photos used in *Google Earth*) could be mistaken with the shoreline when compared with another image. This could lead to erroneous calculations for coastline changes. To implement the necessary adjustment for the tide level, the tide record of the site on a couple of days before and after the image conception was plotted as shown in **Figure 4.2**. The highest tide records for the satellite images are contained in **Table 4.1**.

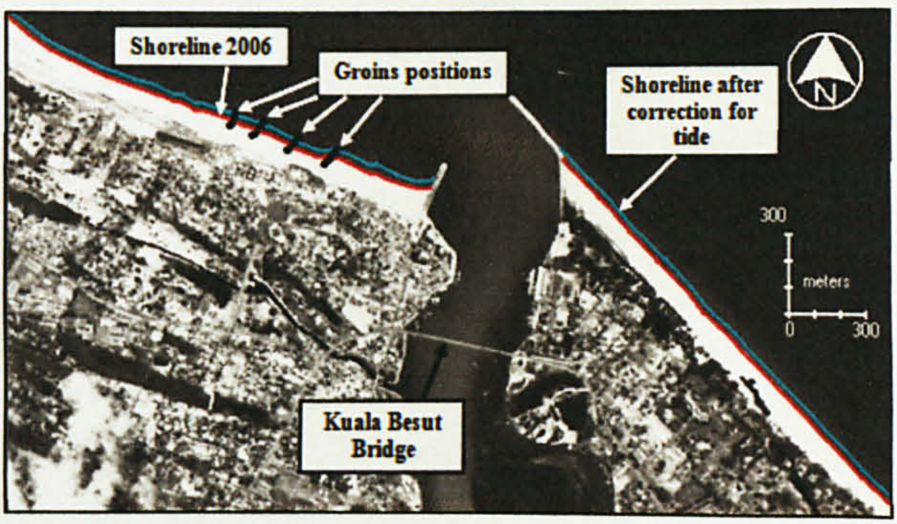

Figure 4.2: Shoreline adjustment for tide levels when the satellite images were taken (applied to 2006-image)

Table 4.1: Tide records for the satellite images

Image Date	Tide Record (m)
03-10-2005	1.30
06-09-2006	1.86
05-09-2007	1.06
03-09-2008	1.54

For example, consider the tide level difference for year 2005 and 2006, and the difference of 1.86–1.30=0.56 m, where the higher tide is associated with the image in 2006. With an average beach slope of 1:40 at the study area, the apparent shoreline of 2006 image should be shifted seaward by 22 m if the images are to be meaningfully overlaid. The tide levels, at specific times when the images are taken, are plotted in **Figure 4.3**.

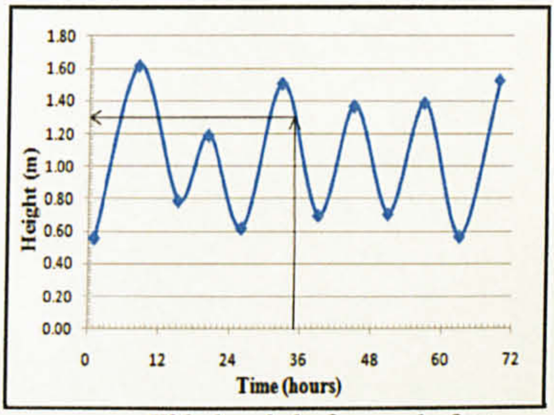

a. Tide levels before and after 3 October 2005

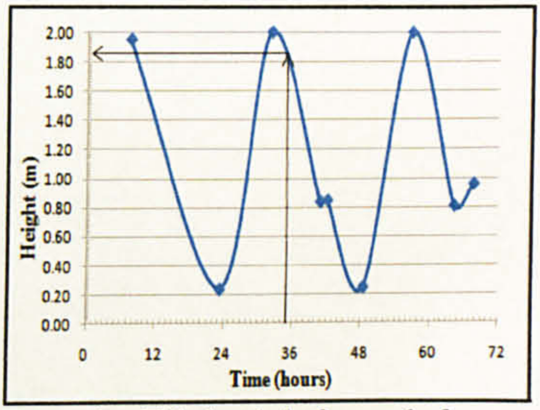

b. Tide levels before and after 6 September 2006

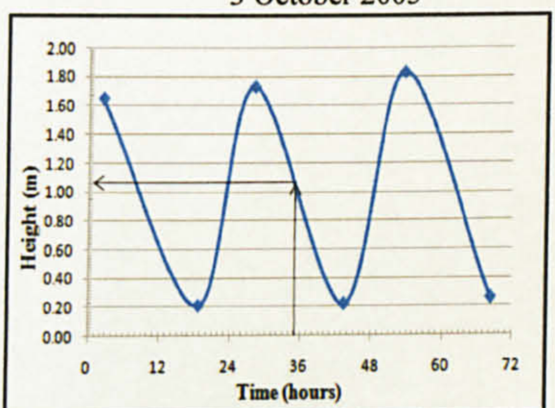

c. Tide levels before and after 5 September 2007

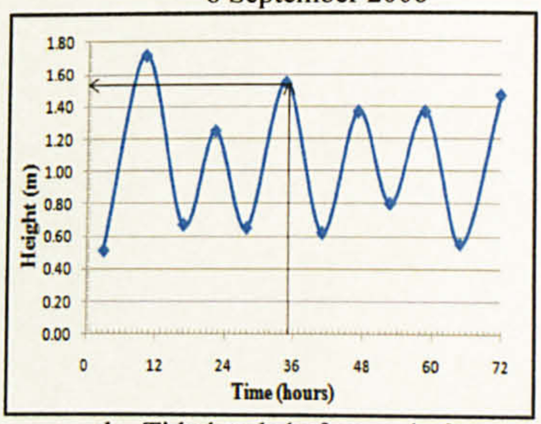

d. Tide levels before and after 3 September 2008

Figure 4.3: Tidal levels at the times the satellite images were taken

The summary of the tide difference for all the images is noted in the **Table 4.2**.

Table 4.2: Summary of tide difference

Tide Comparison	Higher Tide (Year)	Tide Difference (m)	Affected Beach Width (m)
2006-2005	2006	0.56	22
2007-2006	2006	0.80	32
2008-2007	2008	0.48	19
2008-2005	2008	0.24	10

Pairs of images as recorded in Table 4.2 are uploaded in *ERDAS*, processed, overlaid and the shoreline is corrected for the tide levels as shown in **Figures 4.4, 4.5** and **4.6** for both beaches. **Figure 4.7** presents a coastline change from 2005 directly to 2008.

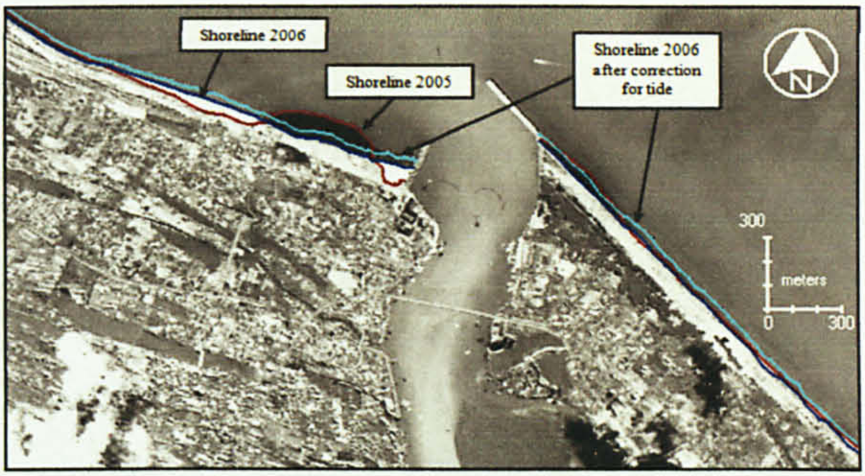

Figure 4.4: Shoreline change from 2005 to 2006 (tide corrected)

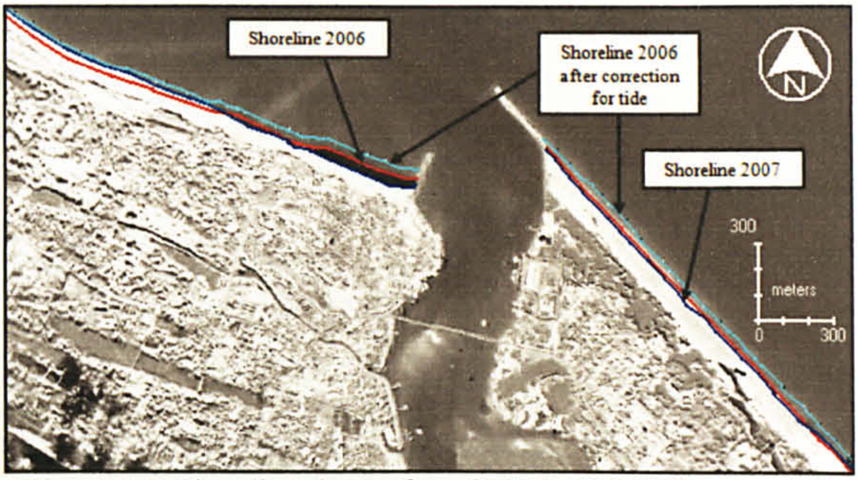

Figure 4.5: Shoreline change from 2006 to 2007 (tide corrected)

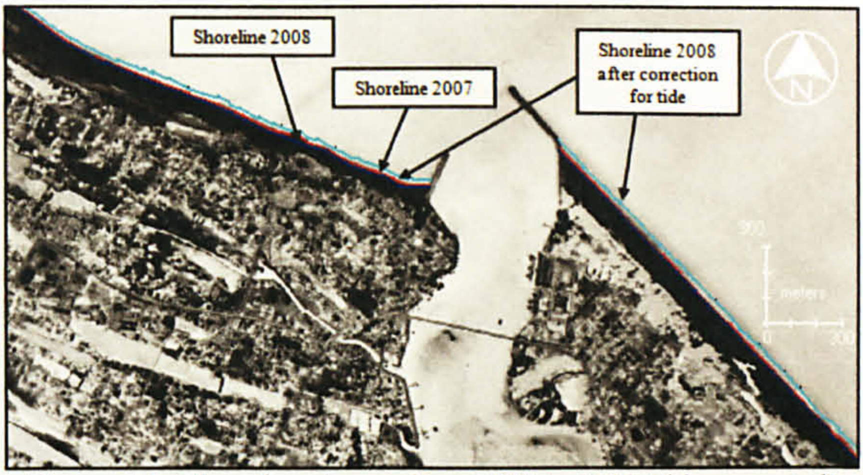

Figure 4.6: Shoreline change from 2007 to 2008 (tide corrected)

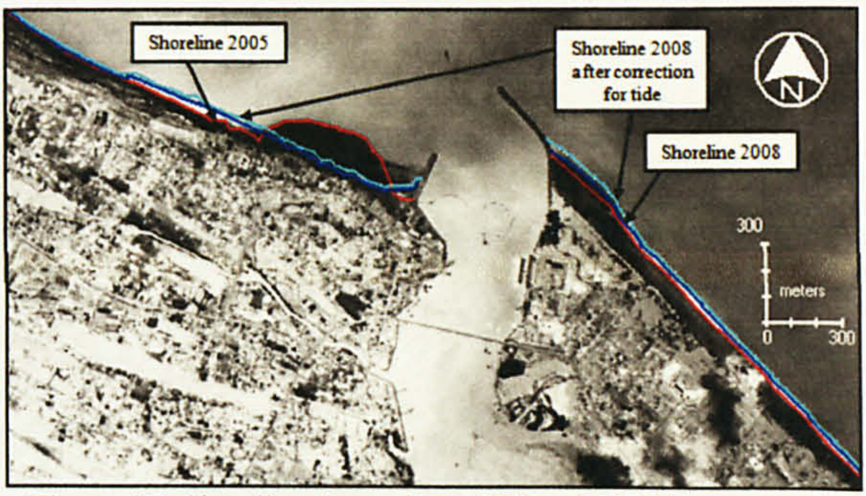

Figure 4.7: Shoreline change from 2005 to 2008 (tide corrected)

The respective areas representing deposition and erosion are computed from the overlaid images. The results are listed in **Table 4.3**.

Table 4.3: Annual change in beach plan area

Beach	Plan Area (ha) 2005-2006	Plan Area (ha) 2006-2007	Plan Area (ha) 2007-2008	Plan Area (ha) 2005-2008
Relevant Figure	Figure 4.4	Figure 4.5	Figure 4.6	Figure 4.7
East (1.8km)	+4.57 -0.29	+0 -4.31	+3.15 -0	+6.13 -0
West (1.8km)	+5.16 -2.44	+0 -4.64	+3.06 -0	+3.35 -5.22
Total (3.6km)	+6.99	-8.95	+6.21	+4.26
Note: "+" means deposition (seaward progress); "-" means erosion				

To give an example, let us consider years 2005 and 2006. The plan view area between the corrected 2006 shoreline and the apparent 2005 shoreline for the east beach (1.8 km of it is shown) represents a net 4.28 ha of deposition that is the algebraic sum of 4.57 ha of deposition and 0.29 ha of local erosion. Considering the beach slope of 1:40, this plan area of 4.28 ha corresponds to the sediment volume of 12,720 m^3 for the east beach contained in a wedge (*i.e.,* a prism with triangular cross-section) with plan area of 4.28 ha, length of 1.8 km and maximum thickness of (42,800/1,800)/40 ≈ 0.60 m. This wedge is 42,000/1,800 ≈ 24 m wide.

4.3 Engineering Estimation of the Coastline Changes

To validate the magnitude of the detected coastline changes, conventional estimation method for longshore sediment transport is employed. The well-known CERC formula as described in the Coastal Engineering Manual (USACE, 2010) is

$$Q = K\sqrt{\frac{g}{k}}\frac{H_b^{2.5}\sin(2\alpha)}{16\,(s-1)(1-n)} \tag{1}$$

where Q is the potential transport in m^3/s, K is a dimensionless coefficient obtained from some empirical equations, H_b is the root-mean-square breaking wave height, k is the breaker index H_b/d_b usually close to 0.9, α is the wave angle with the shore normal, s is the relative density of the sediment (2.65 for quartz), n is the sediment porosity (usually 0.4). In the Shore Protection Manual, SPM, K=0.39 was adopted with H_b replaced by the significant wave height, H_s. Komar in 1988 analysed limited field data and came up with the following simple equation in which D_{50} is in mm.

$$K=1.4 \exp(-2.5\times D_{50}) \quad (2)$$

Table 4.4 contains the data extracted from the wave rose of the North-East Monsoon (November-April; assumed to be five complete months here) as reported in (AIS Consultant, 2009). The wave rose has been reproduced in **Figure 4.8**. The wave rose is constructed from the data reported in 1985 by the famous National Coastline Erosion Study (NCES, 1985).

Table 4.4: Wave heights in various directions

α°	0	0	0	0	0
H (m)	3.75	2.75	1.75	0.75	0.1
Freq.(%)	1.5	4	8	12	5
α°	30	30	30	30	30
H (m)	3.75	2.75	1.75	0.75	0.1
Freq.(%)	1.5	2	8	20	7
αo	60	60	60	60	60
H (m)	3.75	2.75	1.75	0.75	0.1
Freq.(%)	2	2	3	9	4

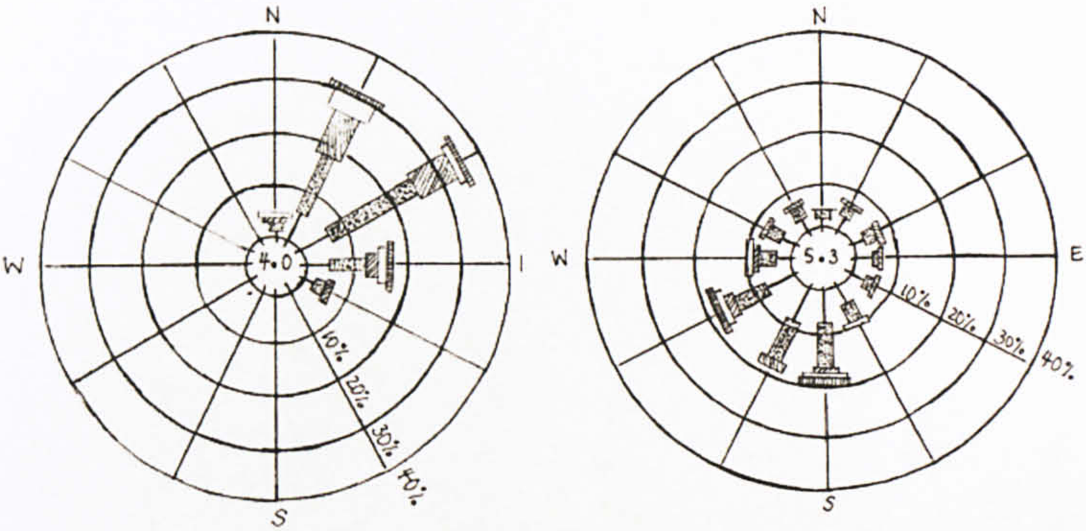

a. North-east monsoon, November- April

b. South-west monsoon, May- October

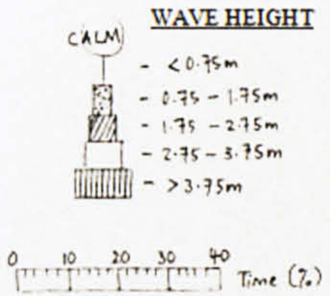

Notes:

1. Wave roses extracted from the National Coastal Erosion Study, Final Report, Volume 1, August 1985
2. Overall period of record: Jan 1943- Dec 1983
3. Source: US National Climate Data Centre, Shipboard Observations
4. Location of Wave Rose- Square A
   Lat. 5° - 8° N   Long. 102° - 107° E

Figure 4.8: Wave rose of the coastal region reproduced from (NCES,1985)

The total of the frequencies reported in Table 4.4 is 89%. The remaining 11% belong to the small waves in ineffective directions such as from SW towards NE. It should be noted that the overall shoreline of the study area (from SE towards NW) makes a 120° with North. The first five waves in Table 4.4 belong to the direction of 60° with N (from NE towards SW) that is normal to the shoreline leading to zero longshore transport along the beach. The wave rose of the South-West Monsoon (May-October) does not lead to any longshore current because of the shoreline direction. This wave rose is not reported and used here.

Based on the results from the sieve analysis, the beach sediment indicates 5-15% clay, 2-25% fine sand, 50-60% medium sand, 15-30% coarse sand with D_{50}=0.36 mm and a corresponding fall velocity of 5 cm/s. The CERC formula is applied to the data with two options for K, one with K_1=0.39 (SPM recommendation) and the other K_2=0.57 resulting from Equation (2). The significant difference is an indication of vulnerability to gross error with the inevitable use of empirical formulae (see p. III-2-17 of CEM in **USACE 30 April 2002 for an example with a 1900% difference). Table 4.5 contains the** results of the calculation for Q_1 (m^3/s) with K_1 and Q_2 (m^3/s) with K_2 for nonzero-angle waves in Table 4.4. In computing Q_t (m^3/yr), the monsoon period is considered 5 months, from mid-November to mid-April.

Table 4.5: Longshore Sediment Transport from CERC

Col. 1	*Col. 2*	*Col. 3*	*Col. 4*	*Col.5*	*Col.6*	*Col.7*
α°	***H* (m)**	**Q_1(m^3/s)**	**Q_2(m^3/s)**	**freq.(%)**	**Q_1(m^3/s) with %** if K_1	**Q_2(m^3/s) with %** if K_2
30	3.75	0.02040	0.02977	1.5	0.03060	0.04465
30	2.75	0.00939	0.01371	2	0.01879	0.02742
30	1.75	0.00303	0.00443	8	0.02428	0.03543
30	0.75	0.00036	0.00053	20	0.00730	0.01065
30	0.25	0.00000	0.00000	7	0.00002	0.00002
60	3.75	0.02020	0.02949	2	0.04041	0.05898
60	2.75	0.00930	0.01358	2	0.01861	0.02716
60	1.75	0.00301	0.00439	3	0.00902	0.01316
60	0.75	0.00036	0.00053	9	0.00325	0.00475
60	0.25	0.00000	0.00000	4	0.00001	0.00001
Total net transport Q_t(m^3/s)					0.22843	0.33339
Total net annual transport Q_t (m^3/yr) considering 5 months (5×24×3600×30)					2.96× 10^6	4.32× 10^6
Transport per meter of beach length assuming a total 60 km of beach (m^3)					49	72
Change in beach width with 1:40 slope					**44 (m)**	**54 (m)**

The columns of Table 4.5 are numbered for ease of reference. *Cols. 6* and *7* are longshore sediment transport as computed by CERC formula with two assumptions for the values for constant K. Algebraic sum of transport rates for all directions yields the total net transport rates (the 1st and 2nd wide rows in Table 4.5). Considering a beach length of 60 km, the transport rate per unit length of the beach is obtained by dividing the total net transport rate by 60000 m (the 3rd wide row in Table 4.5). This is in fact the volume of the sediment contained in a prism 1 m long (along the beach) with a cross-sectional area of $0.5\times x\times(x\times m)$ in which x is the width change (across the beach), m is the beach slope, and $(x\times m)$ is the maximum depth of the erosion or deposition. With beach slope of m=1:40=0.025 and solving for x, the last row of Table 4.5 presents the computed values for x. This is the computed annual beach width change assuming a constant supply of sediment from far south-east direction. Positive value means deposition, applicable to the east beach (ending at the longer breakwater). Where the supply is stopped by the longer breakwater at the end of the east beach, the value is negative indicating erosion, representing the potential transport.

From two final values corresponding to K_1 and K_2, none is to be preferred in the absence of reliable field measurement and observations. Therefore, an average of ≈50 m of the width change is adopted from this estimation.

4.4 Shoreline Classification

A shoreline classification system has been developed for the coasts of Malaysia. The purpose of this system is to define the features of the coastal belt in terms of a limited set of parameters. The primary purpose of the shoreline classification system is basically as a screening device to assist in the identification of the location, length and nature of sections of the coastal belt which can be placed within any item in the set of parameters.

Parameters used to describe the shore are: geomorphology; shoreline condition; coastal processes; shore materials; coastal land use; shore vegetative cover and existing coastal protection structures. **Table 4.6** describes the parameters considered to describe the shore for this study area: the left bank and right bank of Kuala Besut and at outlet of Sg. Besut, Kuala Besut.

Table 4.6: Parameters to describe the shore

Classification Parameters	Location		
	Left bank of Kuala Besut	Kuala Besut	Right bank of Kuala Besut
	Distance = 1.8km	Distance = 0.3km	Distance = 1.8km
Geomorphology	Straight at 120°	River mouth	Straight at 130°
Shoreline Condition	Seasonally Changing	-	Advancing
Coastal Processes	Shore Normal, Shore parallel to the left	-	Shore Normal, Shore parallel to the left
Shore Materials	Quartz Sand	-	Quartz Sand
Coastal Landuse	• Agriculture: coconut plantation, rubber plantation • Towns and developed urban areas • Roadways	-	• Agriculture: coconut plantation • Towns and developed urban areas • Roadways
Shore Vegetative Cover	• Barren lands at shoreline • Grasses, low succulents, low shrubs • Trees • Coconut Trees	-	• Barren lands at shoreline • Grasses, low succulents, low shrubs • Trees • Coconut Trees

The classification parameters are discussed as follows:

1. Geomorphology

The geomorphology of a coastal reach is an all encompass description of the characteristics, origins, and development of coastal land forms. But here the consideration is on the aspect of physical landforms. The 1.8km beach on west of Kuala Besut consists of a stretch of straight shoreline at an angle of 120° followed by the 400m rivermouth and 1.8km beach on east side consists of a straight coastline at angle of 130°.

2. Shoreline Condition

   The shoreline condition is a parameter which describes the shoreline (marine-terestial) interface in terms of erosion. The west beach at Kuala Besut is seasonally changing meanwhile the east coast is an advancing shoreline in the form of the beach accretion.

3. Coastal Process

   The coastal process is the parameter which describes the movement processes of coastal sediments. Both beaches to west and east of Kuala Besut experience shore normal movement and shore parallel to the left movement.

4. Shoreline Materials

   The shoreline materials parameter is simply a description of the material encountered at the shore. For the purposes of aspect of the shoreline classification, the shore is taken as strata (terestial and marine) which are affected by wave energy types of materials. The beaches of Kuala Besut both consists mainly of the quartz sand which are typically sands of alluvial origin or formed from decomposition of coastal lands with a high sand fraction.

5. Shoreline vegetative cover

   The shoreline vegetative cover is taken to be the vegetation (commonly natural) that is found landward of low tide and the undertaking of landuse. Both east and west beaches of Kuala Besut have barren lands at shoreline, also has grasses, low succulents, low shrubs, trees and coconut trees.

6. Coastal Protection Structures

   The coastal structure parameter refers to marine structure which have been constructed solely for the purpose of protecting the shoreline from erosion activity or other structures which either fulfill the same function as a secondary benefit or alternatively have adverse impact on the shoreline. The west beach of Kuala Besut consists of 4 groins and shorter arm of the breakwater. The east beach of Kuala Besut has the longer arm of the breakwater.

4.5 Discussion

The analysis of the coastline changes can efficiently be computed and observed with the application the remote sensing images and interpret them in the remote sensing software. The analysis has actually showed the actual beach width changes throughout 2005-8. The results were presented on the overlaid images in Figures 4.4 to 4.6. The study separated the analysis of the area affected by the beach activities into the east beach and also the west beach. The variation is however not uniform for the activities of the west beach as there are variance in the computational numbers obtained. The net plan area changes along 1.8 km of west beach in intervals 2005-6, 2006-7 and 2007-8 are 2.72 ha, -4.64 ha and 3.05 ha, respectively (Table 4.3).

Along the west beach, the variation is not uniform; neither in time nor in space. There are two obvious reasons for this: The discontinuity because of the river mouth and the groins. The first means interruption to the longshore sediment supply. This could be compensated for partly by the sediment load from the river. In the absence of validated data on the river sediment transport, no quantitative conclusions can be made for the west beach. The second has had a clear impact. The impact can be seen best in Figure 1.9. The groins, built in 2004 (non-existent in Aug-2003 image), captured significant sediment in Jan-Oct 2005, have caused a curious sediment accumulation some time before Oct 2005, and have effectively buried the groins in Oct 2005 and beyond. The data extracted from the images, listed in Table 4.3, reflect a net deposition in the 2005-6 intervals, pronounced erosion in the 2006-7 interval, and a clear deposition in the 2007-8 intervals. In general and as indicated in Figure 4.7, the beach has progressed slightly towards the sea and the groins have become ineffective in capturing the longshore sediment. The yearly fluctuation can be justified by incorporation of river sediment loads (especially that carried by floods) and actual coastal storms. If the estimate of 100,000 m^3/yr of sediment supply from the river is accepted from (AIS Consultants, 2009), it is reasonable to assume that part of this sediment supply deposits at the river mouth ready to be picked up by the longshore currents. Lacking reliable field data, there is not much reading into the estimated numbers related to river mouth sediment. However the lack of the information for the river mouth sediment, there is not much to be commented on the numbers mentioned. Therefore, no attempt is made here to compare the actual beach growth with that from theoretical calculations in Table 4.5.

For the east beach, the situation is clearer. The net plan area changes along 1.8 km in intervals 2005-6, 2006-7 and 2007-8 are 4.28 ha, -4.31 ha and 3.15 ha, respectively (Table 4.3). Dividing the areas by 1800 m yields +24 m, - 24 m, and +18 m, respectively. Comparing these with the computed value of 50 m (Table 4.5) indicates non-uniformity in either the supply (from far SE beaches) or in the function of the long breakwater in capturing the longshore sediment from SE. Moving away from April 1998 (when the breakwaters were built), the long breakwater seems to be inadequate in holding the longshore sediment so that a great portion of the longshore sediment escapes the breakwater to reach the west beach contributing to the continual sediment build up around the groins and beyond. The fact that the orientation of the longer breakwater is inclined along the dominant longshore current (not normal to the west beach) partly explains why it does not trap all the transported sediment along the beach.

4.6 Comparison of the Past and Present

Based on the recent site assessment, some obvious comparisons were observed on the study location comparing to the previous remote sensing images and also present image on Google Earth. Following are some comparisons done based on photos taken at the study location to compare real conditions at site for few different dates respectively. **Figure 4.9** below shows the photos taken at Kuala Besut on 23rd March 2009, 10th July 2009 and 13th May 2010 for the location to the left of the second groin from the left breakwater.

Based on these images, there is a lot of sediment swept to the sea from the shore that gives the cliff difference to the present condition. From 23rd March 2009 to 10th July 2009, there seem to be a lot of sediment lost from the beach. The difference in waterline is also caused be the rise in the sea water level during 10th July 2009. According to the representative from JPS Besut, the previous flood carried off a lot of sediment from the beach. Later during the recent site visit on 13th May 2010, due to the low tide, a lot more beach area is exposed and that causes the difference in the waterline.

a. 23 March 2009

b. 10 July 2009

c. 13 May 2010

Figure 4.9: Photos taken to the left of the second groin from the left breakwater

Comparison can also be done for the location behind the left breakwater on 10th July 2009 and also 13th May 2010 as shown in **Figure 4.10**. The difference for this location can also be summarized due to the difference in tide levels that gives such an impression for waterline and shore profile difference.

a. 10 July 2009 b. 13 May 2010

Figure 4.10: Photos taken behind the left breakwater

Figure 4.11 gives an overall impression of comparison for 23rd March 2009 to 13th May 2010 for location next to the right breakwater considering both of these days having nearly the same tide levels. Here it can be observed that sediment has been transported off the beach for comparison near the waterline. The beach level was much higher with more sediment during 23rd March 2009.

a. 23 March 2009 b. 13 May 2010

Figure 4.11: Photos taken next to right breakwater

Based the comparison of the remote sensing images to the latest image of 2nd August 2005 from Google Earth, the conclusion is that the two images of different resolution gives different impression to analyze the sediment movement. This is acceptable for the coastline changes as an overall but lacks the information to comparison of sediment movement. The current condition of the site is acceptable as of 2nd August 2005 image from the Google Earth, except that during the site visit, there were some obvious changes such as the number of groins on the site.

The structures produced at the site are by Jabatan Kerja Raya (JKR) as some supplementary structure to block the longshore sediment transport. There were 8 groins (**Figure 4.12**) observed on the site compared to 4 groins from the satellite images (Figure 1.4).

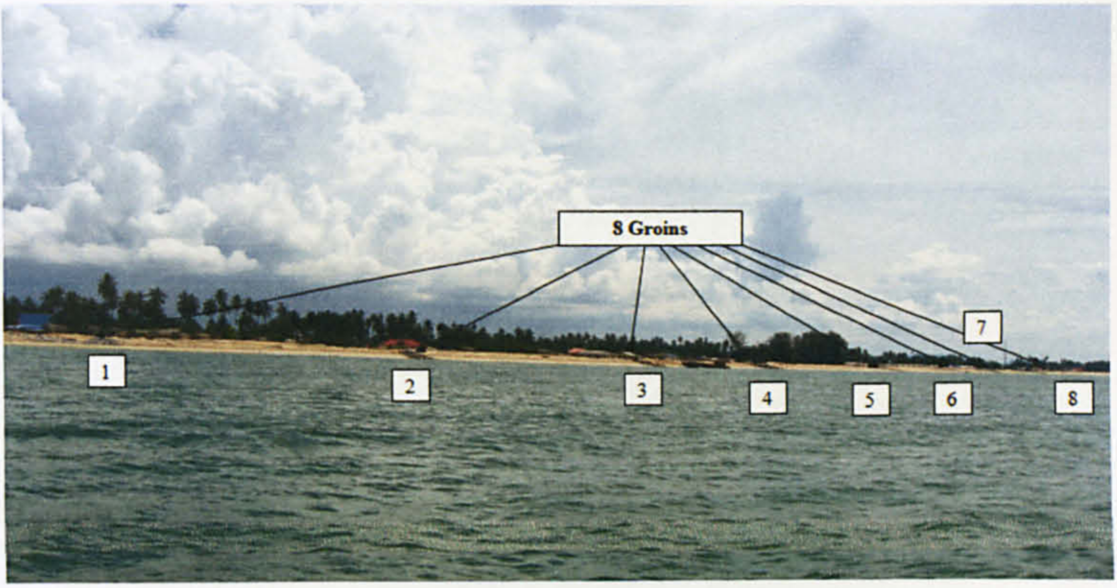

Figure 4.12: Eight groins at Kuala Besut

Based on the knowledge and observations during the site visit, the impact of tide on the difference in the waterline can really affect the interpretation of the images and analysis to understand longshore sediment transport. This is an important aspect to look into for analysis of coastline changes as has been discussed in the study. It also points out also the importance of satellite image analysis and site assessment.

CHAPTER 5

CONCLUSION AND RECOMMENDATION

The coastline changes on a 4-km-stretch of an active beach in Terengganu, Malaysia, was adopted by using the remote sensing images with the help of the remote sensing software for change detection analysis. The coastline is interrupted by the river mouth of Sg. Besut. Four *x-y* satellite images, 4 years apart, were processed and overlaid in GIS software. The shorelines were adjusted to incorporate the effect of the tide levels on the apparent position of the shoreline. From the beach slope and the migration of the shorelines, volumes of the erosion and deposition were computed and compared with estimates from the application of the longshore transport formula, CERC. The following conclusions can be drawn from this exercise.

1. Incorporating the tide level, at the time the image was taken, into the shoreline is essential if two or more images are to be overlaid and compared. Neglecting this tide level correction will lead to gross errors in computation of the actual migration of the shoreline.
2. Given the gross approximation inherent in sediment motion computation in coastal waters, the results from two methods for the east beach (south east of the longer breakwater) were considered close enough. As the main purpose of the study is to introduce a framework for the simple application of *x-y* images, caution was practiced not read too much into the estimates in this case study.
3. In both image processing and CERC methods, the estimate of the sediment volume corresponding to the shoreline migration is greatly sensitive to the beach slope. To minimise the errors stemming from wrong assumptions for the beach slope, a reliable value of the beach slope should be used. This should come from either field survey or the usage of DEM data containing information on the elevation.

CHAPTER 6

ECONOMIC BENEFITS

A summary project statement of economic costs and benefits is required as the basis for project decisions. Both costs and benefits should be valued at constant economic prices. The statement needs to be drawn up for each subproject, for each project alternative, and for a project as a whole. The statement will differ between projects. However, some common conventions are used to represent the different types of cost and benefit over the life of the project.

For the case of this project, since it involves study and analysis, the cost involves the *ERDAS Imagine ® V9.1* software, and also remote sensing satellite images. Besides that, to work further into the analysis using Digitized Elevation Model (DEM), there is also consideration of the data purchasing cost.

The restricted remote sensing images from Remote Sensing Agency Malaysia will cost up to RM1000 per image. To purchase the DEM data it will also cost up to RM2000 per data. However, for the case of this study since it is used for study purposes, the author was not charged for any details and data by the government agency.

However, for the case if this study is done by other parties, they have to consider purchasing the software and work on it. Besides that, the images will be charged and reasoning has to be given when the images are purchased by individuals or private companies. This study is still considered as cost saving as it will be much cheaper to perform the study than to prepare modeling or appointing other parties to perform the analysis. This study can be performed in-house by any individual by learning the suitable software and processing the images.

REFERENCES

Abdullah, D. I. (1993). Director General, Department of Irrigation and Drainage, Malaysia. *Coastal Developments in Malaysia- Scope, Issues, and Challenges* .

About Us: Jabatan Pengairan dan Saliran . (2008). Retrieved October 20, 2009, from Laman Web Rasmi Jabatan Pengairan dan Saliran : http://www.water.gov.my/

AIS Consultants, 2009, Investigation on Rehabilitation Works in Sungai Besut Coast in Terengganu, Report submitted to the Department of Public Works, Malaysia

B. Shaw, a. J. (1995). *Survey of multispectral methods for land cover change analysis:*

Chalabi, A., Mohd-Lokman, H., Mohd-Suffian, I., Karamali, M., 2004, Geomorphological features of Kuala Terengganu Spit from IKONOS Imagery and Aerial Photographs Using Segmentation Method online from http://www.aars-acrs.org/acrs/prooceeding/ACRS2005/Papers/CSZ2-4.pdf

Chalabi A, Mohd-Lokman H, Mohd-Suffian I, Karamali K, Karthigeyan V., Masita M., 2006, Monitoring shoreline change using IKONOS image and aerial photographs: A case study of Kuala Terengganu area, Malaysia, *ISPRS Midterm Symposium Proceeding*, May, Enschede, The Netherlands.

DeWitt, H. W., 2002, *Semi-automated construction of the Louisiana coastline digital land-water Boundary using Landsat TM imagery*, Louisiana's Oil Spill Research and Development Program.

Frihy O.E., S. N. (1995). *Remote sensing of Beach Erosion Along the Rosetta Promotary, Northwestern Nile delta Egypt. Int. J. Remote Sensing* , 1649-1660.

Ghosh, C. (1995). *Identificationof the cause of Coastal Erosion at Digha,India by Remote Sensing* .

Gorman L., Morang A., Larson R., 1998, Monitoring the Coastal Environment; Part IV: Mapping, Shorline Changes, and Bathymetric Analysis, *Journal of Coastal Research*, 14(1), 61-92.

Hennecke W.G., 2004, GIS modeling of sea-level rise induced shoreline changes inside coastal re-entrants- two examples from southeastern Australia, *Natural Hazards*, 31(1), pp. 253–276.

Ibrahim Z.A, 2009, Investigations on Coastline changes of North Terengganu, Final Year Project, *Universiti Teknologi PETRONAS*

J.Y., C. L. (1998). International Journal of Remote Sensing. *Detection of Shoreline Changes for tideland areas using multi- temporal satellite images , 19* (17), 3383- 3397.

Karsli, F. A. (2003). Monitoring Coastal Land USe Changes on the Turkish Black Sea Coast with Remote Sensing: An Example from Trabzon, Turkey. *2nd FIG Regional Conference* . Marrakech, Morocco: TS7 Coastal Zone Management.

Kumarasivam Tan & Ariffin Sd. Bhd., 1987, Besut Flood Mitigation Project, Final Project, Volume 1: main Report, Report submitted to the Department of Public Works, Malaysia.

Kumarasivam Tan & Ariffin Sdn. Bhd., July 1988, Besut Flood Mitigation Project, Final Report, Volume 2; Supporting Appendices to Main Report, Report submitted to the Department of Public Works, Malaysia.

Larson R, Morang A., Gorman L., 1997, Monitoring the Coastal Environment; Part II: Sediment Sampling and Geotechnical Methods, *Journal of Coastal Research*, 13(2), 308-330.

Li X., Y. A. (1998). International Journal of Remote Sensing . *Principal component analysis of stacked multi- temporal images for the monitoring of rapid urban expansion in the Pearl River Delta , 19* (8), 1501- 1518.

Lokman M.H., Rosnan Y., Shahbudin S., 1995, Beach Erosion Variability during a Northeast Monsoon: the Kuala Setiu Coastline, Terengganu, Malaysia, Pertanika *J. Sci. & Technol.*, Vol. 3 No. 2, 337-348

Li R., Liu J-K, Felus Y., 2001, Spatial Modeling and Analysis for Shoreline Change Detection and Coastal Erosion Monitoring, *Marine Geodesy*, 1521-060X, Vol. 24, Issue 1, pp 1–12.

Maged Marphany, S. M. (1998). *Shoreline Change Detection using TOPSAR/AIRSAR Data .*

Mazlan, H. I. (1989). *Preliminary Evaluation of Photogrammetric-remote sensing Approach in Monitoring Shoreline Erosion .*

Morang A., Larson R., L Gorman A., 1997, Monitoring the coastal environment; Part I: Waves and currents, *Journal of Coastal Research*, 13(1), 111-133.

Morang A., Larson R., Gorman L, 1997, Monitoring the Coastal Environment; Part III: Geophysical and Research Methods, *Journal of Coastal Research*, 13(4), 1064-1085

Raj, J. (1982). *Net Directions and Rates of Presentday Beach Sediment Transport by Littoral Drift along the East Coast of Peninsular Malaysia* (15), 57-82.

Rongxing Li, J.-K. L. (2000). *Spatial Modeling and Analysis for Shoreline Change Detection and Coastal Erosion Monitoring .*

Rosnan Y., Hussein M.L., Tajudin A., 1995, Variation of Beach Sand in relation to Littoral Drift along the Kuala Terengganu Coast, *Geol. Soc. Malaysia*, Buletin 58, December, 71-78

Saied Choopani, H. H. (2000). *Investigation of Kouhestak- Karian Coastline Changes using GIS.*

SATO S, 2000, Sediment Transport and Beach Profile Change Due to Random Waves, in *Handbook of Coastal Engineering* by John B. Herbich (ed), Chapter 7, McGraw-Hill.

Singh, A., 1989, Digital change detection techniques using remotely- sensed data, International Journal of Remote Sensing, 10(6): 989-1003.

Stanley Consultants, Inc., 1985, *National Coastal Erosion Study* Final Report Volumes I and II, Economic Planning Unit, Prime Minister's Department, Malaysia.

Townshnd, J.R.G., C.O. Justice, C. Gurney, and J Mc Manus, 1992, The Impact of mis-registration in change detection, IEEE Transactions on Geoscience and Remote Sensing, 30(5): 1054-1060.

USACE (U.S. Army Corps of Engineers), 2010, *Coastal Engineering Manual: Overview andCoastal Hydrodynamics,* Engineer Manual EM 1110-21100, Change 2 (2008), Don C. Warrington.

Zakariya R., Rosnan ,Y., Saidin S.A., Yahya, M. H., Kasawani, I., Lokman, H., 2006, 'Shoreline detection and change for Terengganu River Mouth from Satellite Imagery (Landsat 5 and Landsat 7)', *Journal of Sustainability Science and Management*, 1(1):47-57

Zhu, X. (2001). Remote Sensing Monitoring of Coastline Chnage in Pearl River Estuary. *22nd Asian Conference on Remote Sensing* . Singapore.

APPENDICES

Appendix 1

Table A1: List of Coastal Erosion Areas in Malaysia

State	Length of Coastline (km)	Length of Coastline Having Erosion			Total Length of Coastline having Erosion	
		Category 1	Category 2	Category 3		
		CRITICAL EROSION (km)	SIGNIFICANT EROSION (km)	ACCEPTABLE EROSION (km)	(km)	(%)
PERLIS	20	4.4	3.7	6.4	14.5	72.50
KEDAH	148	31.4	2.2	6.9	43.5	29.40
PULAU PINANG	152	42.4	19.7	1.1	53.2	41.60
PERAK	230	28.3	18.8	93.1	140.2	61.00
SELANGOR	213	63.5	22.3	66.1	151.9	71.30
N. SEMBILAN	58	3.9	7.7	12.9	24.5	42.20
MELAKA	73	15.6	15.1	6	36.7	50.30
JOHOR	492	28.9	50.3	155.6	234.8	47.70
PAHANG	271	12.4	5.2	37.6	52.1	73.4
TERENGGANU	244	20	10	122.4	152.4	62.50
KELANTAN	71	5	9.5	37.6	52.1	73.40
W. P. LABUAN	59	2.5	3	25.1	30.6	51.90
SARAWAK	1035	17.3	22.3	9.6	49.2	4.80
SABAH	1743	12.8	3.5	279.2	295.5	17.00
TOTAL	**4809**	**288.4**	**193.3**	**932.8**	**1 415**	**29.41**
		6.0 %	**4.0 %**	**19.4 %**		

Source: Annual Report, Department of Irrigation and Drainage (DID) Malaysia (2007)

Appendix 2

Table A2: Summary of Eroding Coastlines in Malaysia

Region	Total Length of Coast (km)	Category 1	Category 2	Category 3	Total Length of eroding coastline (km)	Percentage
Peninsular	1972	131 (41)	213 (57)	651 (58)	995 (156)	73%
Sabah	1802	6 (3)	10 (7)	310 (14)	326 (24)	24%
Sarawak	1035	8 (3)	23 (11)	14 (7)	45 (21)	3%
Total	4809	145 (47)	246 (75)	975 (79)	1366 (201)	100%

( ) Number of sites

Appendix 3

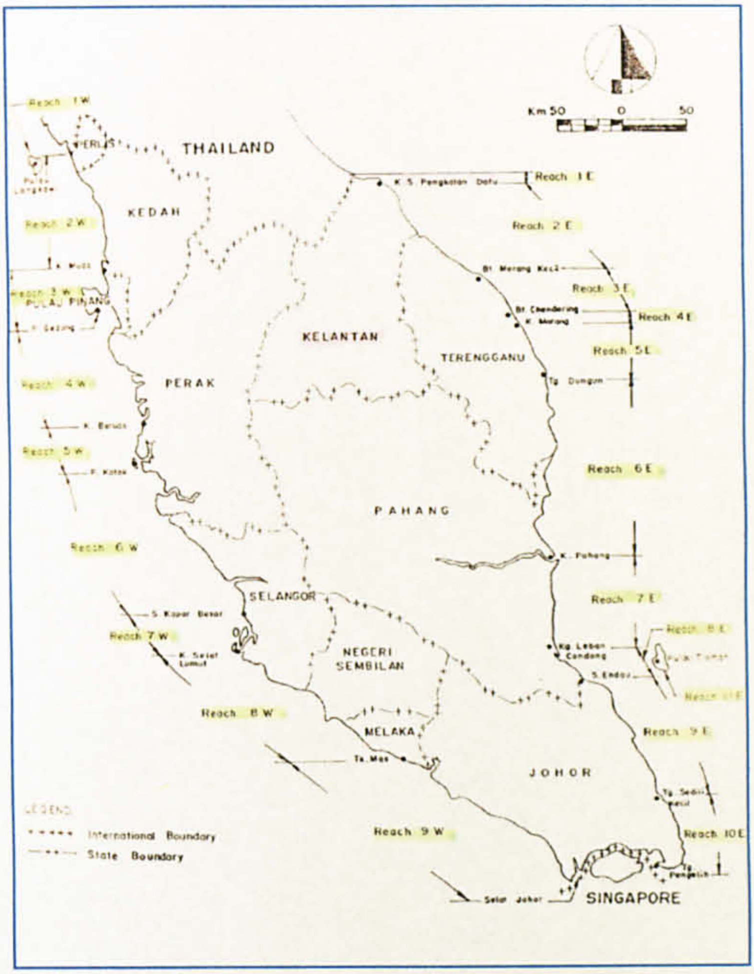

Source: National Coastal Erosion Study 1985, Volume 2

Figure A3: Coastal reaches of Peninsular Malaysia

Appendix 4

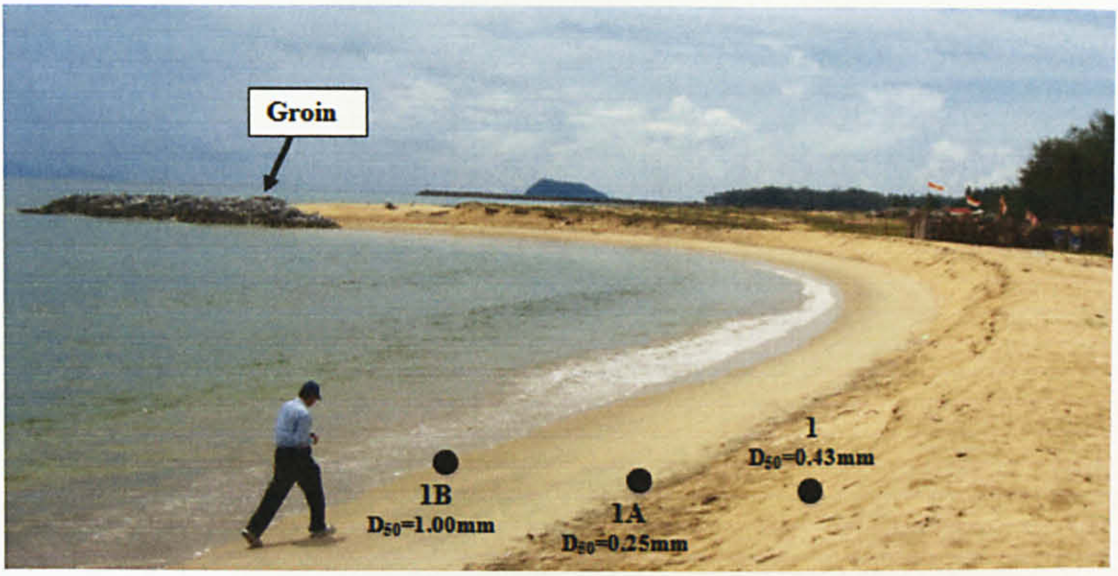

Figure A4.1: Sample locations before the 2nd groin from the left breakwater

Figure A4.2: Sample locations between the 1st groin and the 2nd groin nearing the left breakwater

Figure A4.3: Sample locations behind the left breakwater

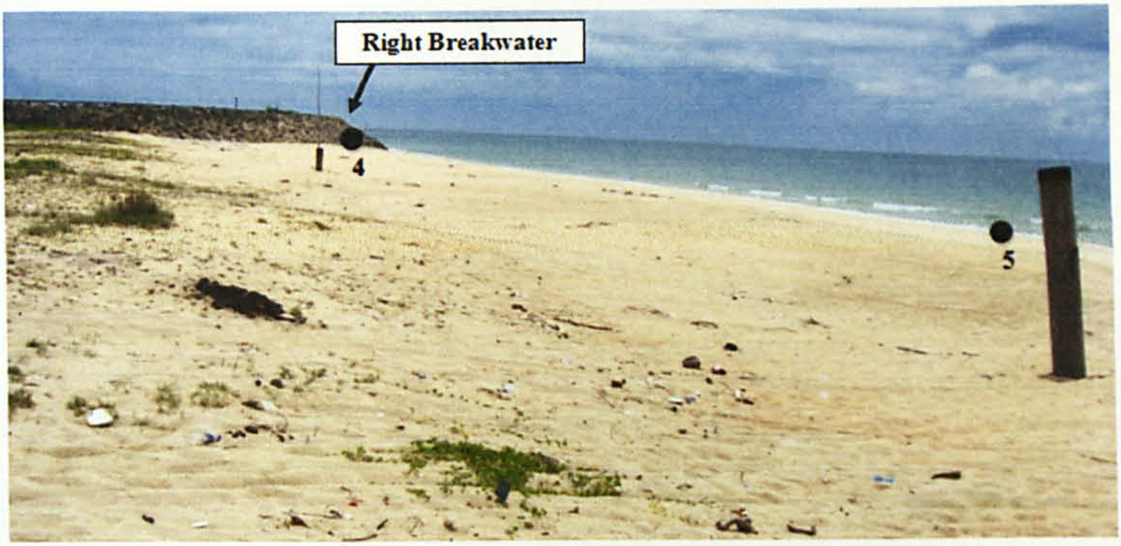

Figure A4.4: Sample locations behind the right breakwater

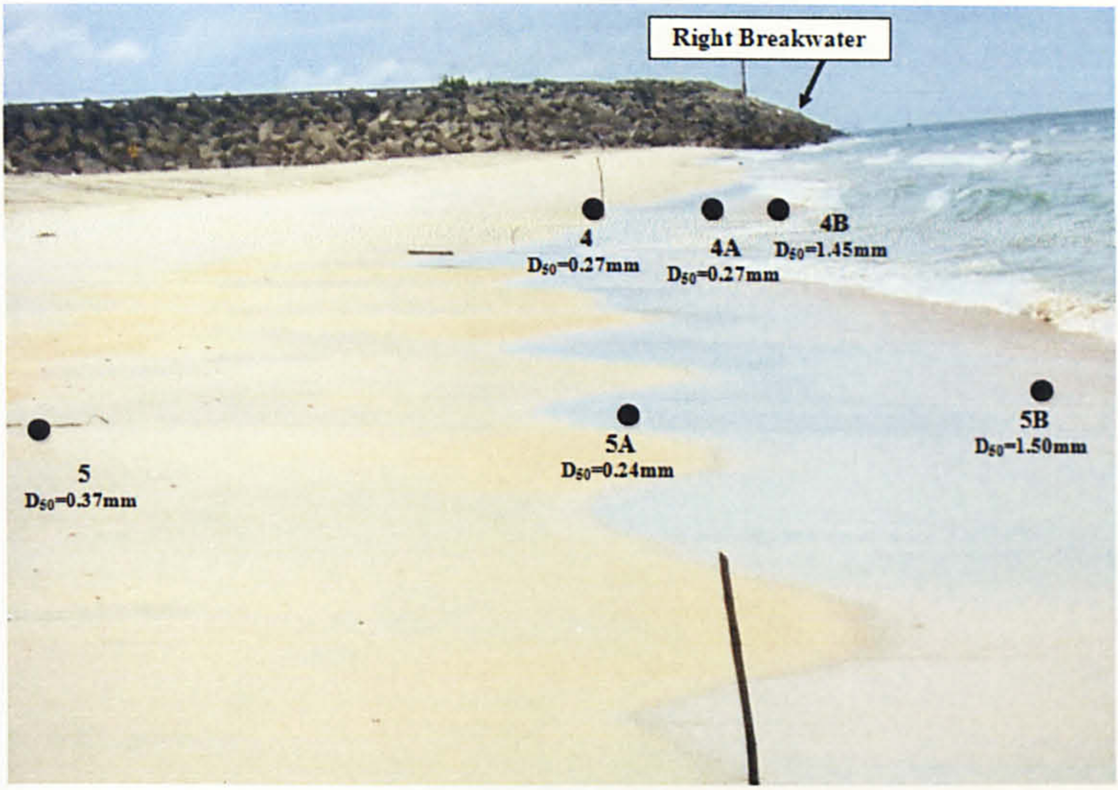

Figure A4.5: Sample Locations after the right breakwater

Figure A4.6: Sample locations after the right breakwater towards area of final surveying

Appendix 5

Table A5.1: Result of Sieve Analysis for Location 1

Sieve Size	Sample 1		Sample 1A		Sample 1B	
	Mass Passing	% Passing	Mass Passing	% Passing	Mass Passing	% Passing
3.35mm	500.0	100.0	500.0	100.0	455.9	91.2
2.00mm	496.4	99.3	499.9	100.0	386.6	77.3
1.18mm	475.6	95.1	499.0	99.8	291.1	58.2
600μm	382.0	76.4	490.9	98.2	155.5	31.1
425μm	253.6	50.7	462.5	92.5	112.6	22.5
300μm	96.4	19.3	331.6	66.3	73.8	14.8
212μm	14.9	3.0	166.5	33.3	49.8	10.0
150μm	4.1	0.8	48.9	9.8	25.3	5.1
63μm	0.3	0.1	1.3	0.3	0.3	0.1
pan	0.0	0.0	0.0	0.0	0.0	0.0

Table A5.2: Result of Sieve Analysis for Location 2

Sieve Size	Sample 2		Sample 2A		Sample 2B	
	Mass Passing	% Passing	Mass Passing	% Passing	Mass Passing	% Passing
3.35mm	500.0	100.0	500.0	100.0	484.3	96.9
2.00mm	499.8	100.0	494.7	98.9	448.3	89.7
1.18mm	470.3	94.1	447.0	89.4	384.5	76.9
600μm	260.9	52.2	325.6	65.1	286.5	57.3
425μm	191.5	38.3	282.9	56.6	244.6	48.9
300μm	106.2	21.2	224.2	44.8	186.1	37.2
212μm	47.6	9.5	133.5	26.7	119.2	23.8
150μm	12.4	2.5	33.9	6.8	45.3	9.1
63μm	0.1	0.0	0.7	0.1	0.9	0.2
pan	0.0	0.0	0.0	0.0	0.0	0.0

Table A5.3: Result of Sieve Analysis for Location 3

Sieve Size	Sample 3		Sample 3A	
	Mass Passing	% Passing	Mass Passing	% Passing
3.35mm	499.6	99.9	498.8	99.8
2.00mm	494.7	98.9	490.4	98.1
1.18mm	461.8	92.4	451.5	90.3
600μm	334.9	67.0	259.4	51.9
425μm	287.0	57.4	204.1	40.8
300μm	242.0	48.4	188.7	37.7
212μm	154.3	30.9	178.3	35.7
150μm	63.2	12.6	157.6	31.5
63μm	3.3	0.7	9.3	1.9
pan	0.0	0.0	0.0	0.0

Table A5.4: Result of Sieve Analysis for Location 4

Sieve Size	Sample 4		Sample 4A		Sample 4B	
	Mass Passing	% Passing	Mass Passing	% Passing	Mass Passing	% Passing
3.35mm	500.0	100.0	499.8	100.0	486.8	97.4
2.00mm	499.9	100.0	498.5	99.7	398.8	79.8
1.18mm	493.7	98.7	480.6	96.1	202.4	40.5
600μm	455.3	91.1	434.0	86.8	84.7	16.9
425μm	418.4	83.7	400.8	80.2	61.1	12.2
300μm	316.0	63.2	304.3	60.9	47.2	9.4
212μm	96.4	19.3	94.9	19.0	25.1	5.0
150μm	13.4	2.7	18.2	3.6	6.9	1.4
63μm	0.1	0.0	0.1	0.0	0.1	0.0
pan	0.0	0.0	0.0	0.0	0.0	0.0

Table A5.5: Result of Sieve Analysis for Location 5

Sieve Size	Sample 5		Sample 5A		Sample 5B	
	Mass Passing	% Passing	Mass Passing	% Passing	Mass Passing	% Passing
3.35mm	500.0	100.0	499.9	100.0	482.2	96.4
2.00mm	500.0	100.0	499.7	99.9	369.1	73.8
1.18mm	499.1	99.8	498.5	99.7	185.8	37.2
600μm	480.5	96.1	483.9	96.8	104.1	20.8
425μm	439.3	87.9	459.5	91.9	90.2	18.0
300μm	302.2	60.4	387.3	77.5	73.1	14.6
212μm	79.5	15.9	184.7	36.9	47.7	9.5
150μm	9.9	2.0	29.0	5.8	17.9	3.6
63μm	0.0	0.0	0.9	0.2	0.1	0.0
pan	0.0	0.0	0.0	0.0	0.0	0.0

Table A5.6: Result of Sieve Analysis for Location 6

Sieve Size	Sample 6		Sample 6A		Sample 6B	
	Mass Passing	% Passing	Mass Passing	% Passing	Mass Passing	% Passing
3.35mm	500.0	100.0	499.1	99.8	499.6	99.9
2.00mm	499.3	99.9	498.7	99.7	491.9	98.4
1.18mm	490.6	98.1	498.0	99.6	465.7	93.1
600μm	449.7	89.9	495.8	99.2	394.7	78.9
425μm	389.9	78.0	491.3	98.3	349.5	69.9
300μm	238.4	47.7	474.2	94.8	269.4	53.9
212μm	60.2	12.0	223.7	44.7	133.9	26.8
150μm	5.9	1.2	43.3	8.7	40.0	8.0
63μm	0.0	0.0	0.7	0.1	1.0	0.2
pan	0.0	0.0	0.0	0.0	0.0	0.0

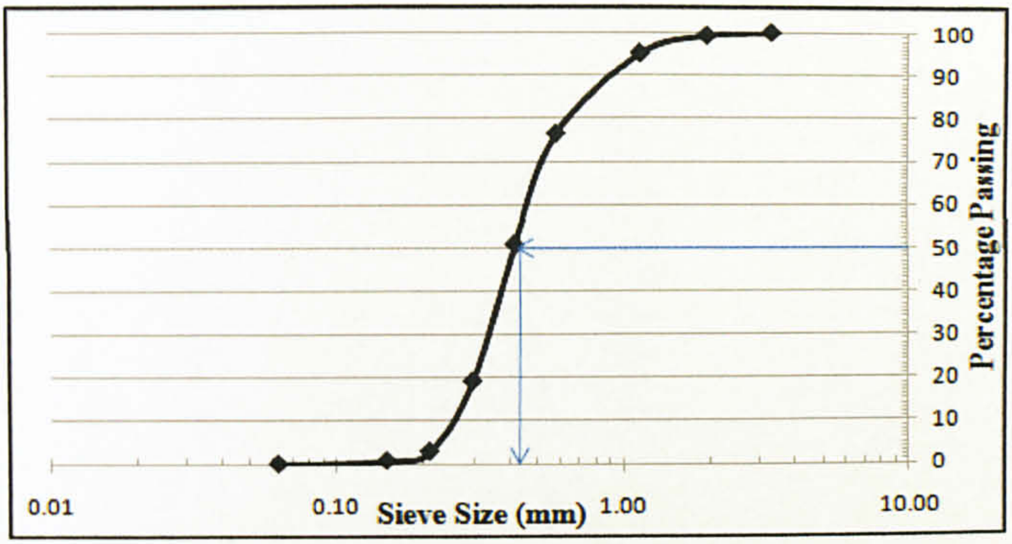

Figure A5.1: Gradation Curve for Sediment Sample 1

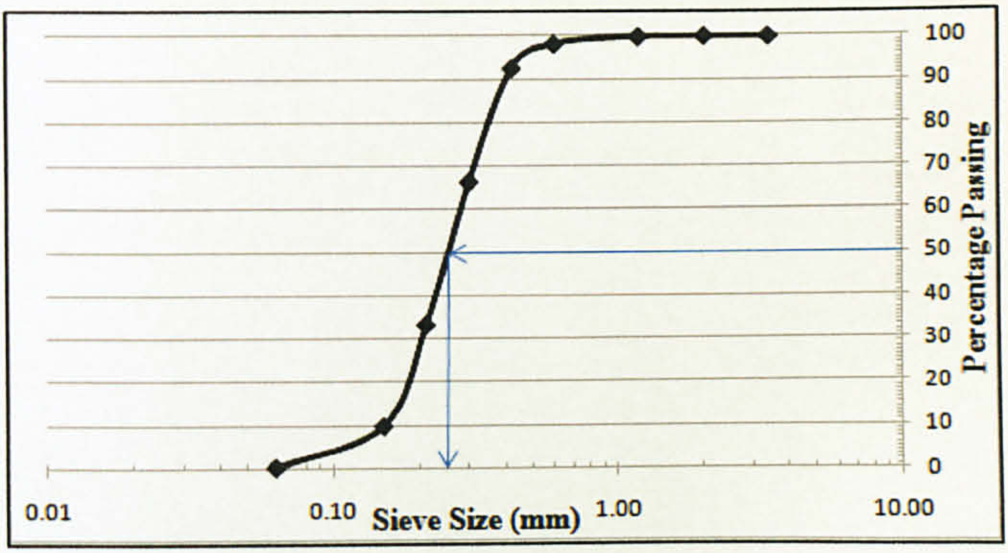

Figure A5.2: Gradation Curve for Sediment Sample 1A

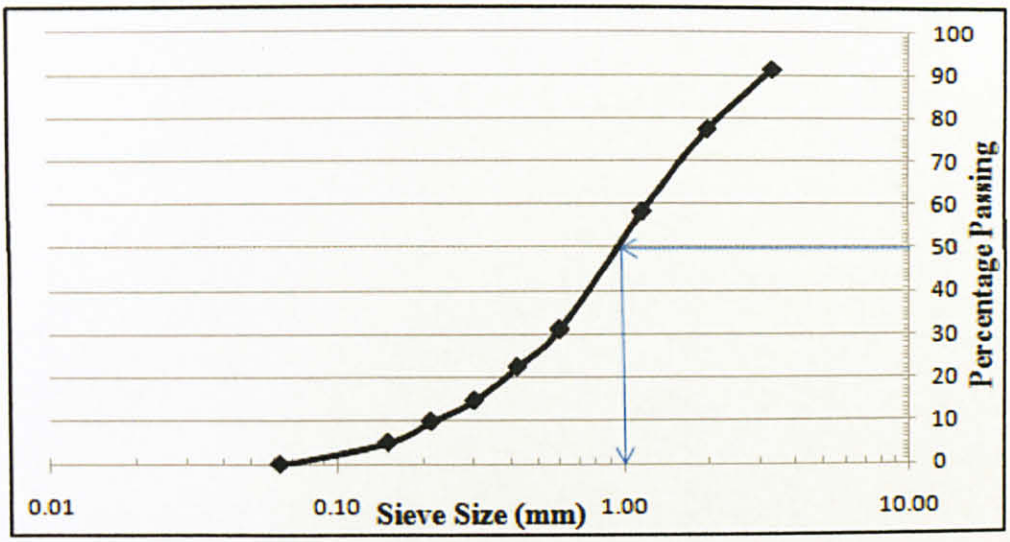

Figure A5.3: Gradation Curve for Sediment Sample 1B

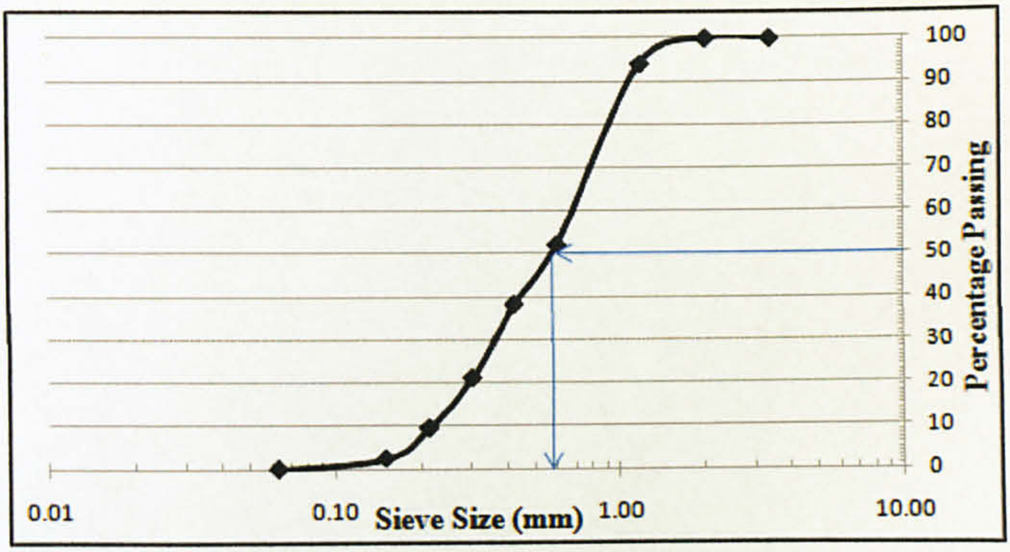

Figure A5.4: Gradation Curve for Sediment Sample 2

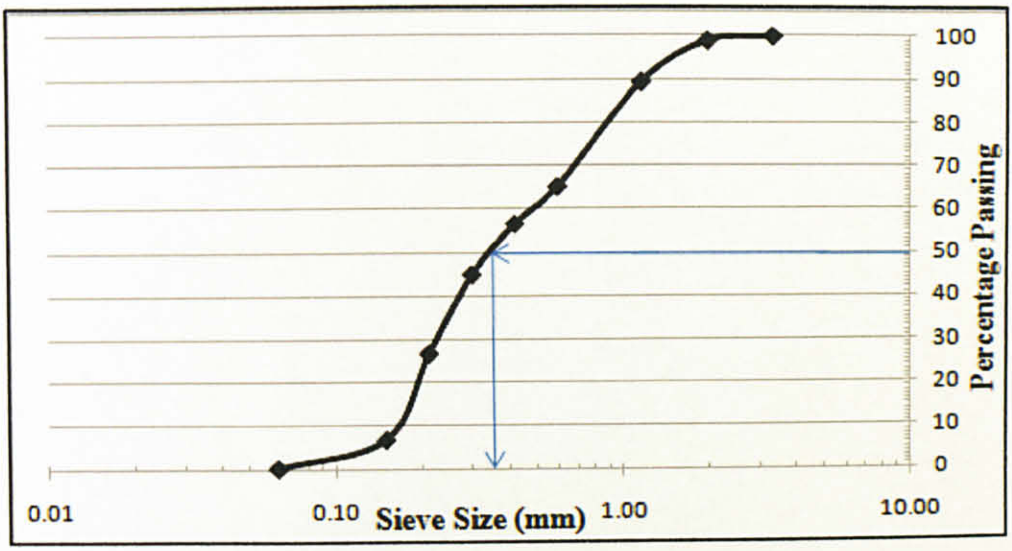

Figure A5.5: Gradation Curve for Sediment Sample 2A

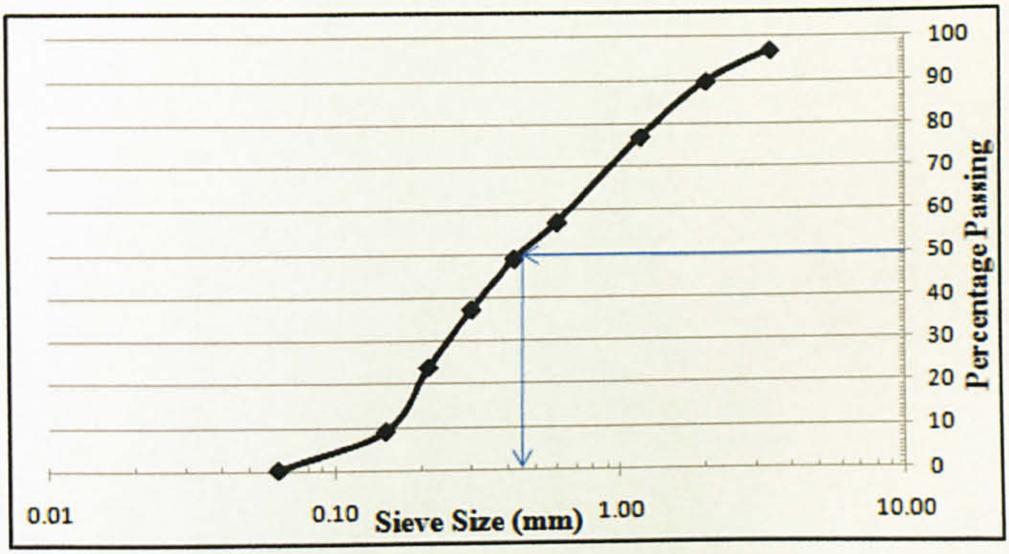

Figure A5.6: Gradation Curve for Sediment Sample 2B

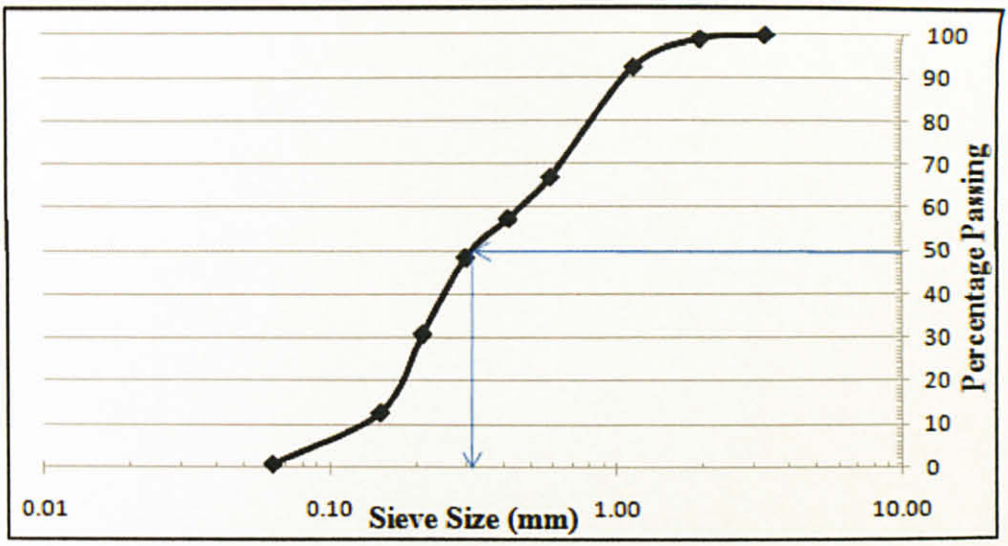

Figure A5.7: Gradation Curve for Sediment Sample 3

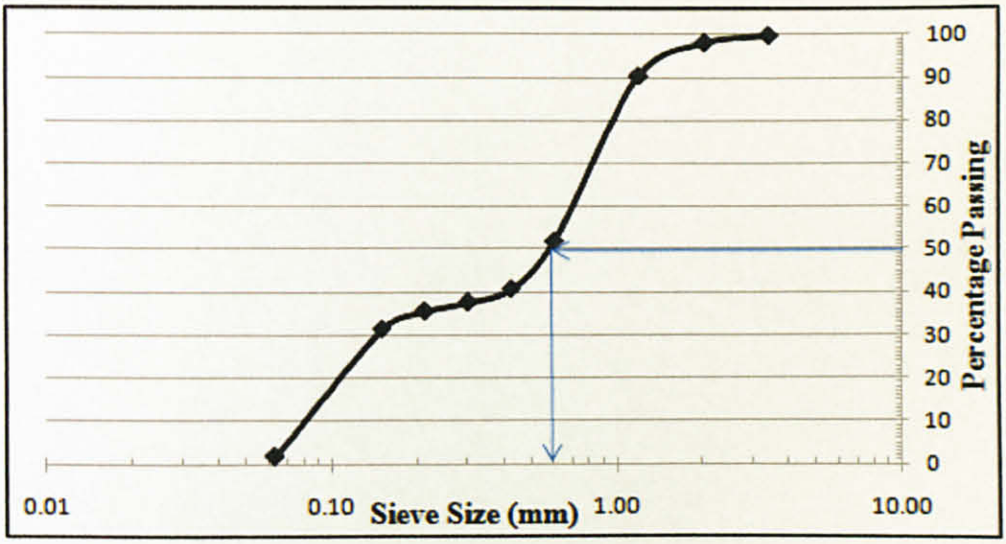

Figure A5.8: Gradation Curve for Sediment Sample 3A

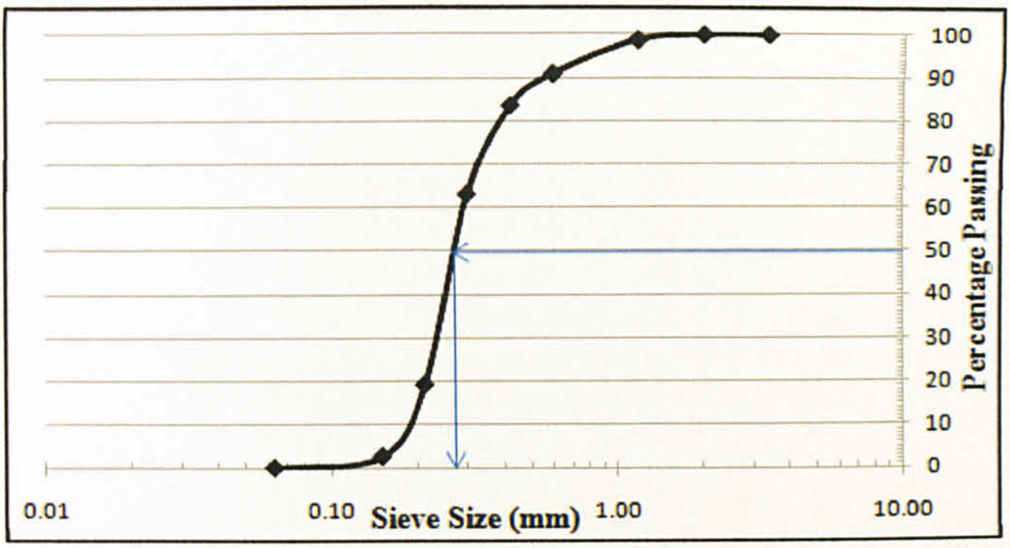

Figure A5.9: Gradation Curve for Sediment Sample 4

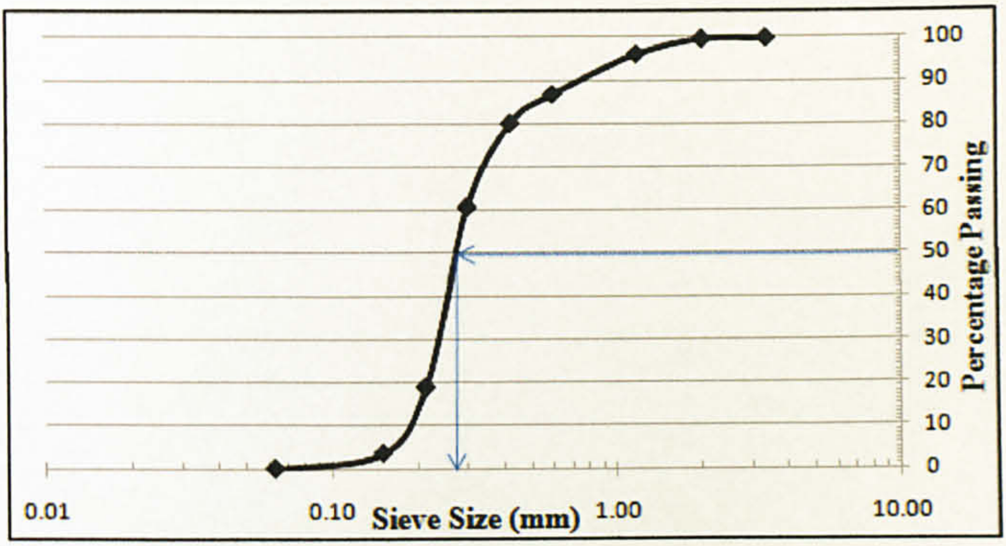

Figure A5.10: Gradation Curve for Sediment Sample 4A

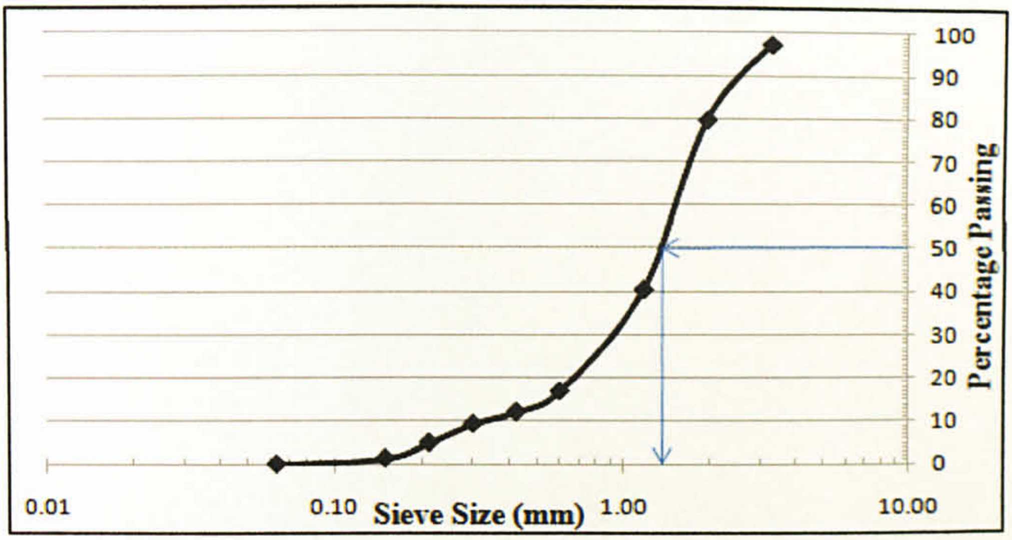

Figure A5.11: Gradation Curve for Sediment Sample 4B

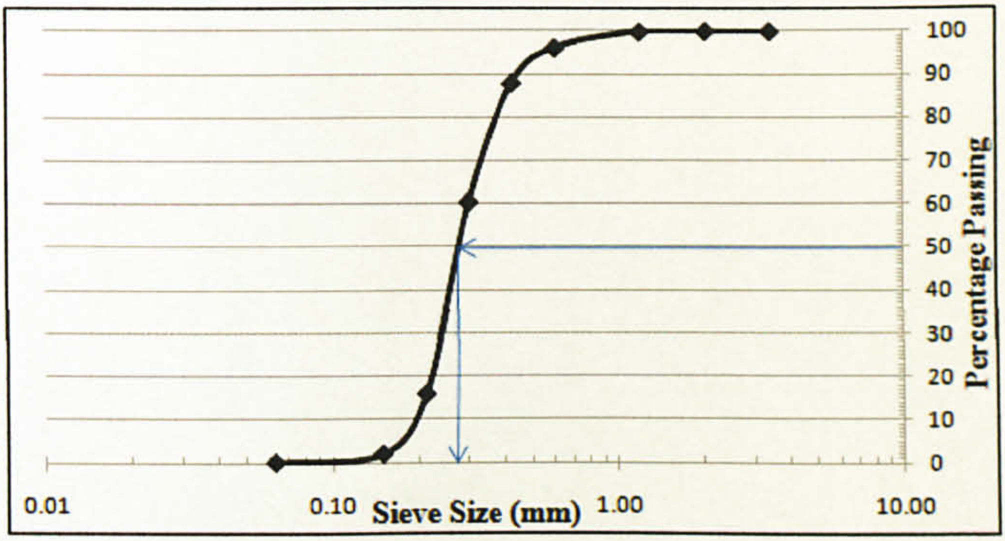

Figure A5.12: Gradation Curve for Sediment Sample 5

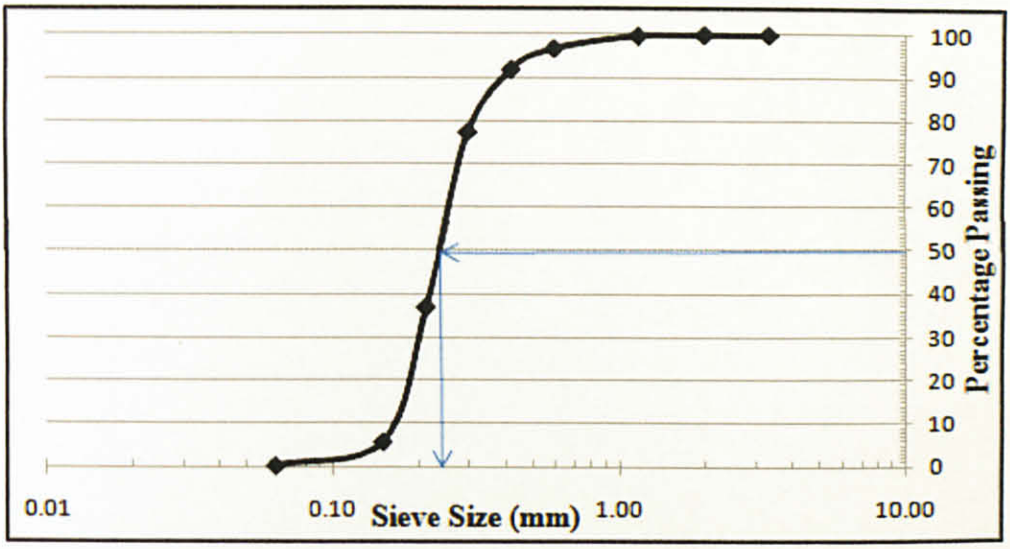

Figure A5.13: Gradation Curve for Sediment Sample 5A

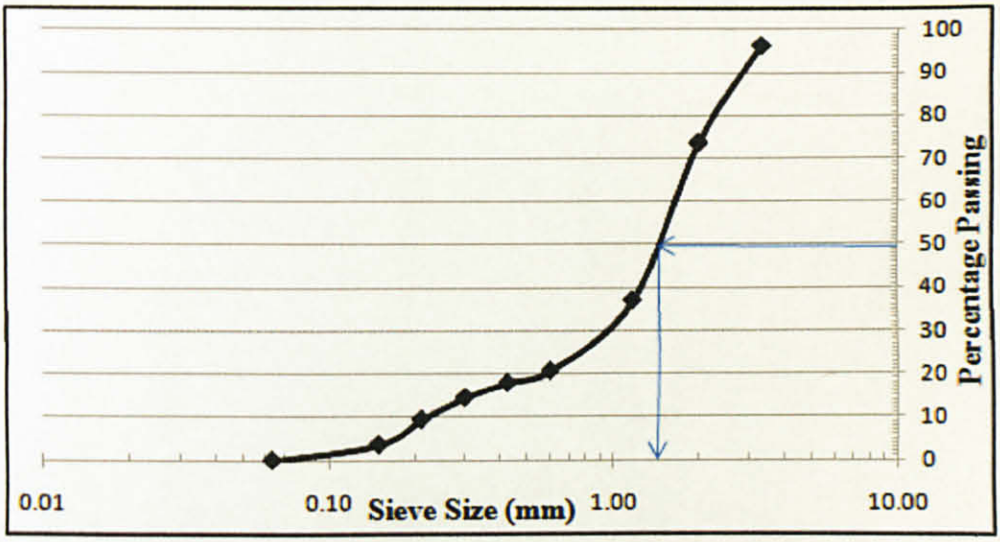

Figure A5.14: Gradation Curve for Sediment Sample 5B

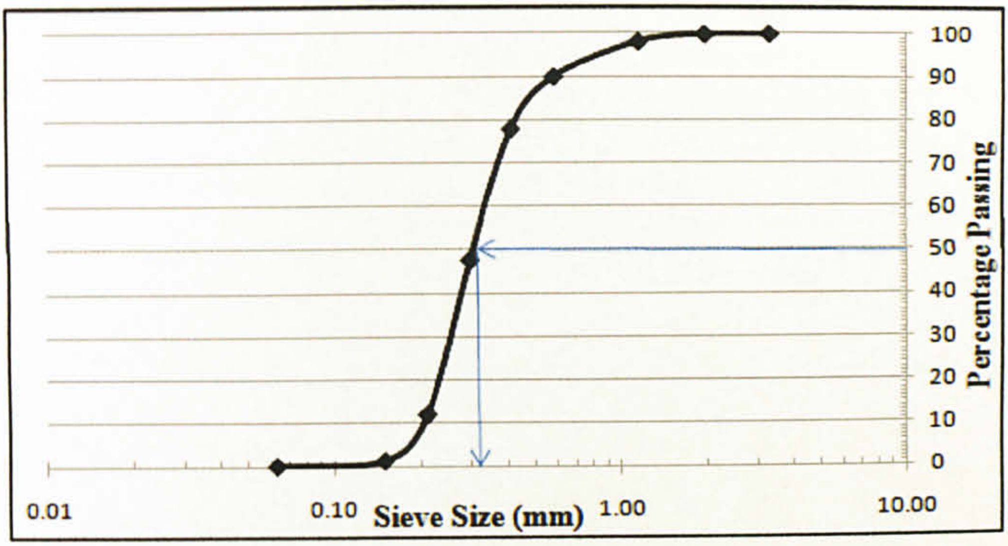

Figure A5.15: Gradation Curve for Sediment Sample 6

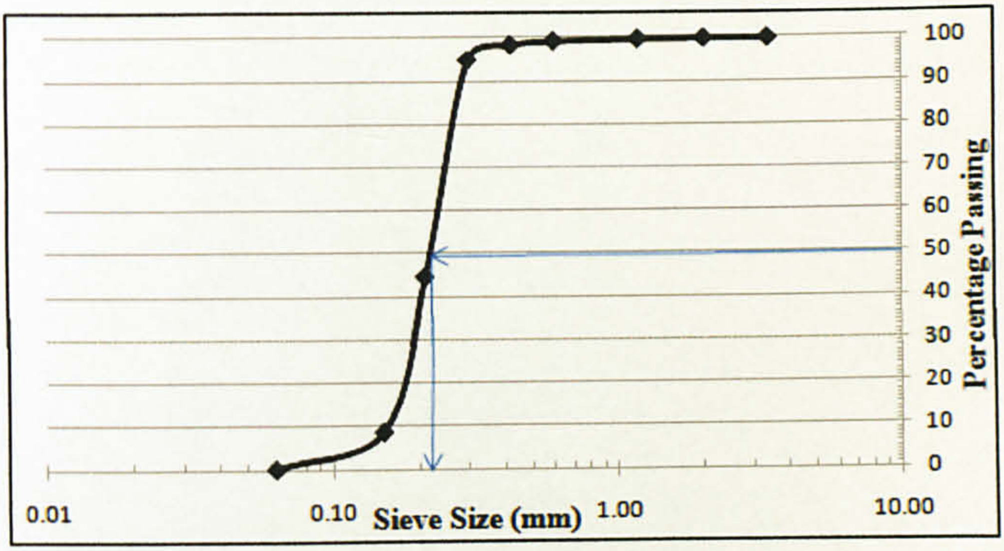

Figure A5.16: Gradation Curve for Sediment Sample 6A

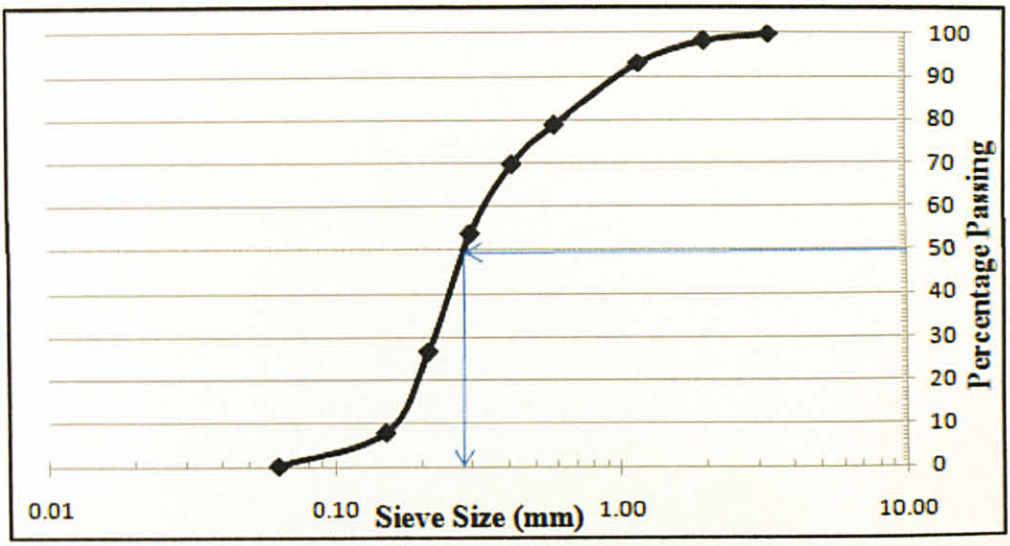

Figure A5.17: Gradation Curve for Sediment Sample 6B

Appendix 6

Table A6.1: Computation of beach slope for Location 1

Points	**Location 1**			
	1000	1050	1051	1052
x	1212.13	1197.84	1177.04	1142.6
y	941.147	939.319	937.898	930.878
z	97.979	98.959	99.594	99.868

Table A6.2: Computation of beach slope for Location 2

Points	**Location 2**			
	1005	1046	1047	1053
x	1138.85	1135.94	1131.17	1124.05
y	971.592	966.724	957.171	939.853
z	98.004	98.52	99.42	99.762

Table A6.3: Computation of beach slope for Location 3

Points	**Location 3**			
	1007	1040	1041	1056
x	1083.91	1081.6	1076.02	1065.98
y	998.513	991.636	979.884	969.424
z	98.077	98.569	99.42	99.662

Table A6.4: Computation of beach slope for Location 4

Points	**Location 4**			
	1010	1031	2025	2026
x	1002.26	999.33	994.634	988.718
y	1033.87	1028.41	1016.26	1003.69
z	98.45	98.563	99.355	100.097

Table A6.5: Computation of beach slope for Location 5

Points	Location 5			
	1013	1023	2019	1061
x	923.617	922.424	912.923	915.121
y	1069.16	1063.45	1044.87	1037.48
z	98.105	98.733	100.117	100.138

Table A6.6: Computation of beach slope for Location 6

Points	Location 6			
	2011	1016	1017	1062
x	860.395	855.472	850.321	844.345
y	1116.5	1095.94	1085.52	1068.73
z	98.356	98.617	99.351	100.339

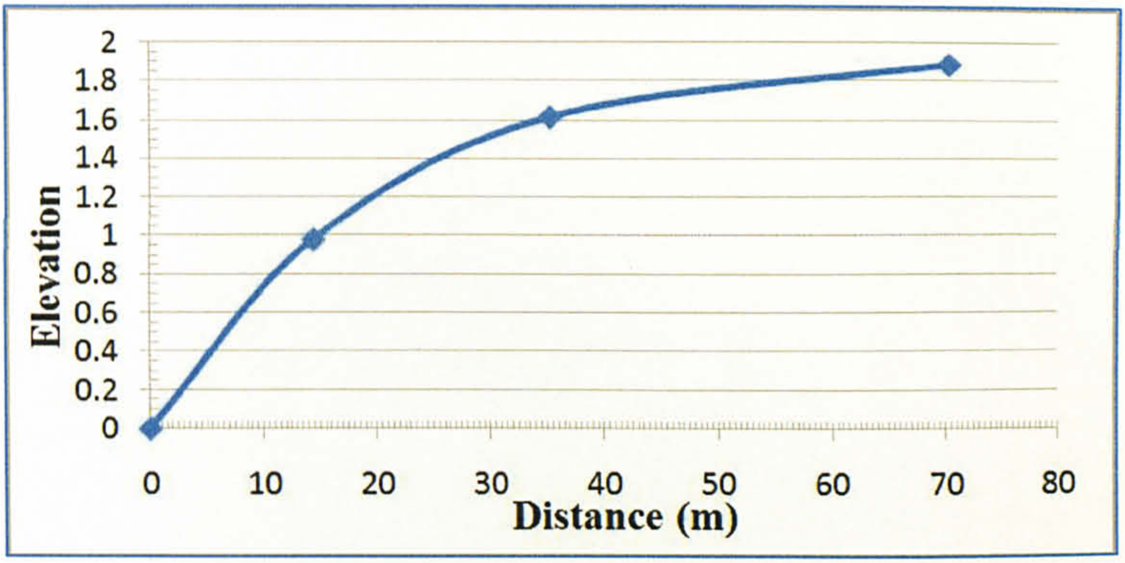

Figure A6.1: Plot for beach slope Location 1

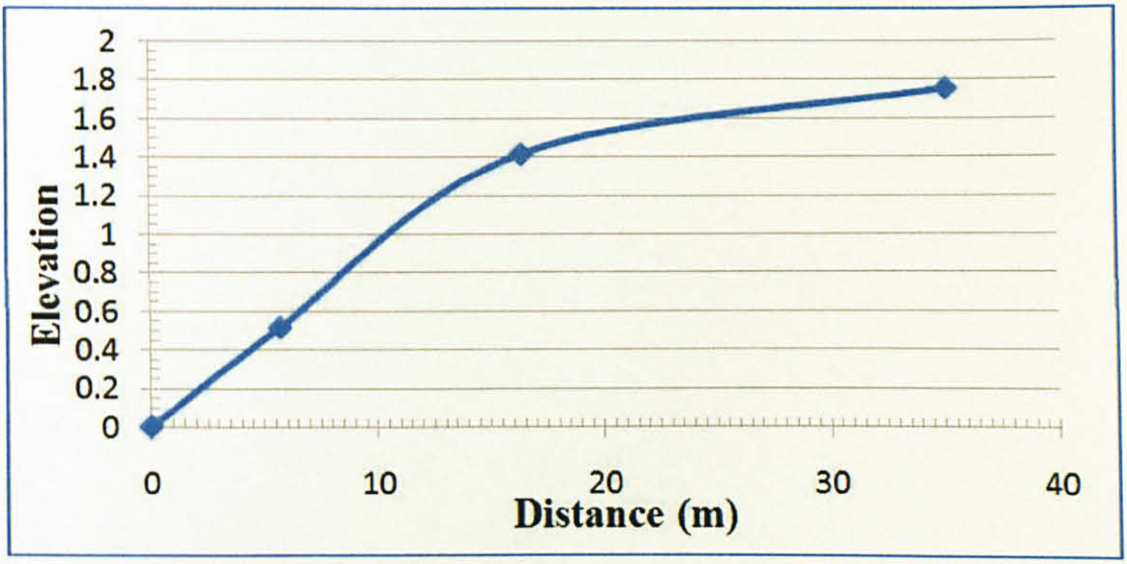

Figure A6.2: Plot for beach slope Location 2

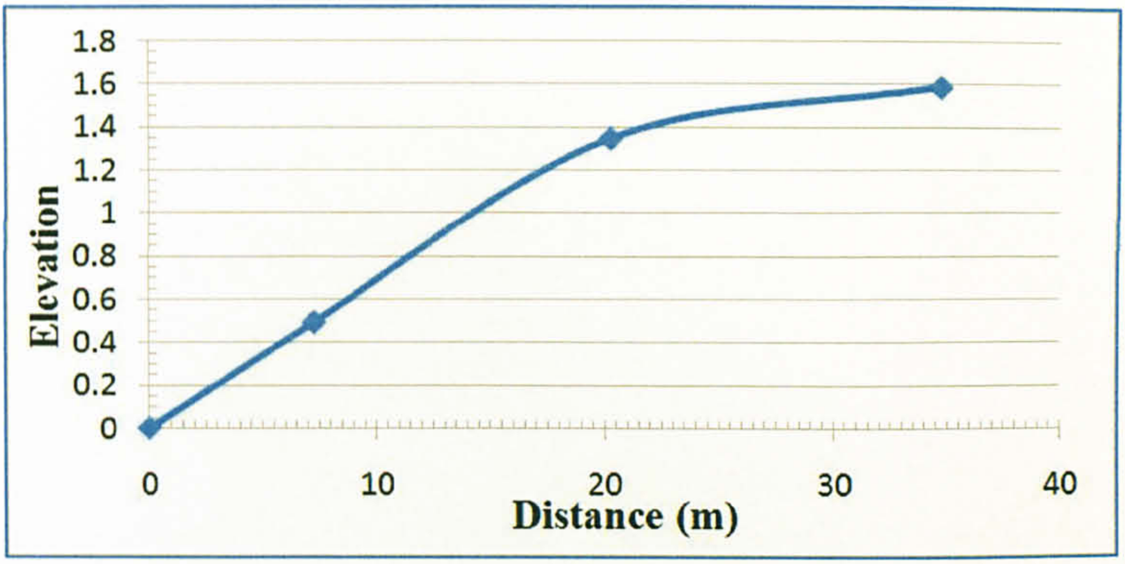

Figure A6.3: Plot for beach slope Location 3

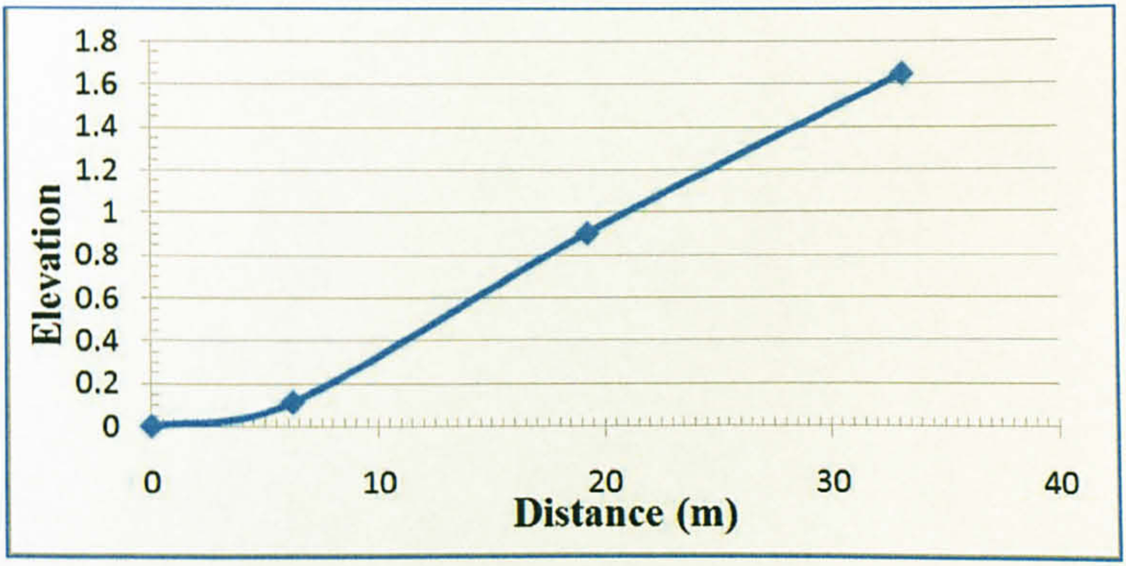

Figure A6.4: Plot for beach slope Location 4

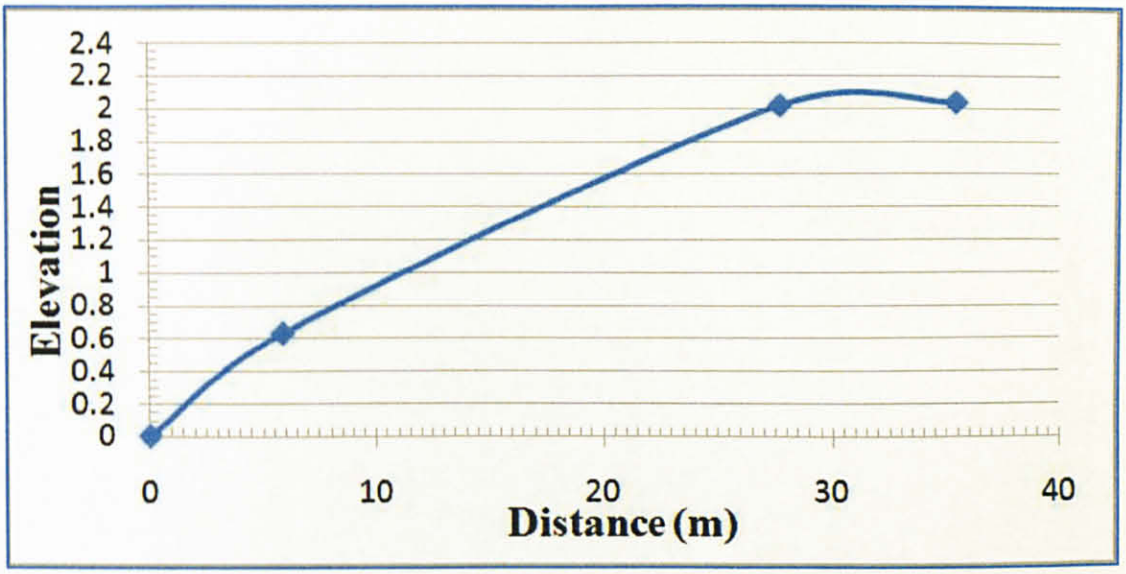

Figure A6.5: Plot for beach slope Location 5

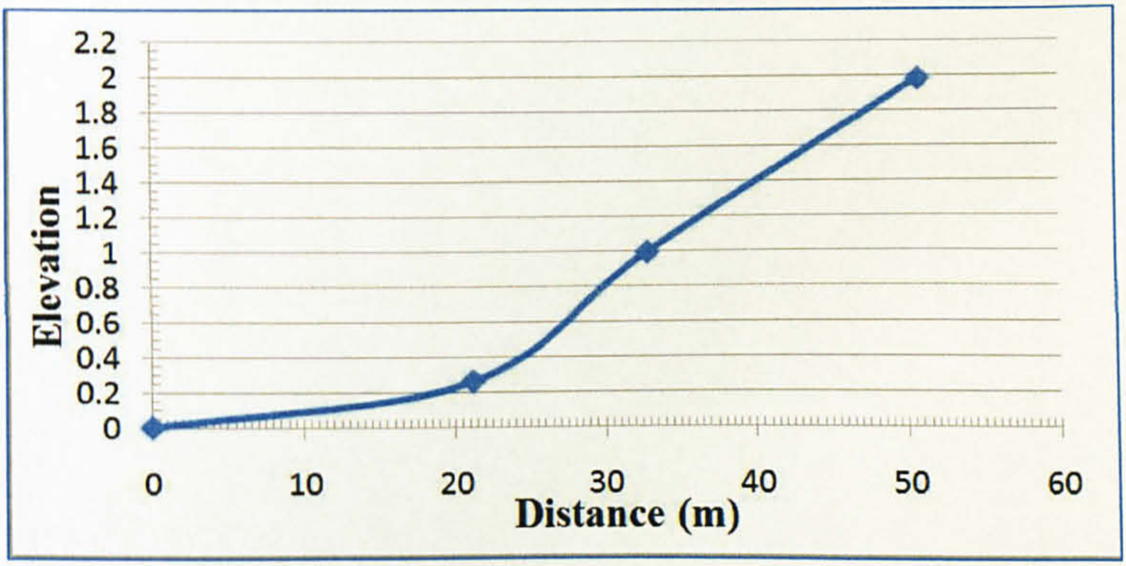

Figure A6.6: Plot for beach slope Location 6

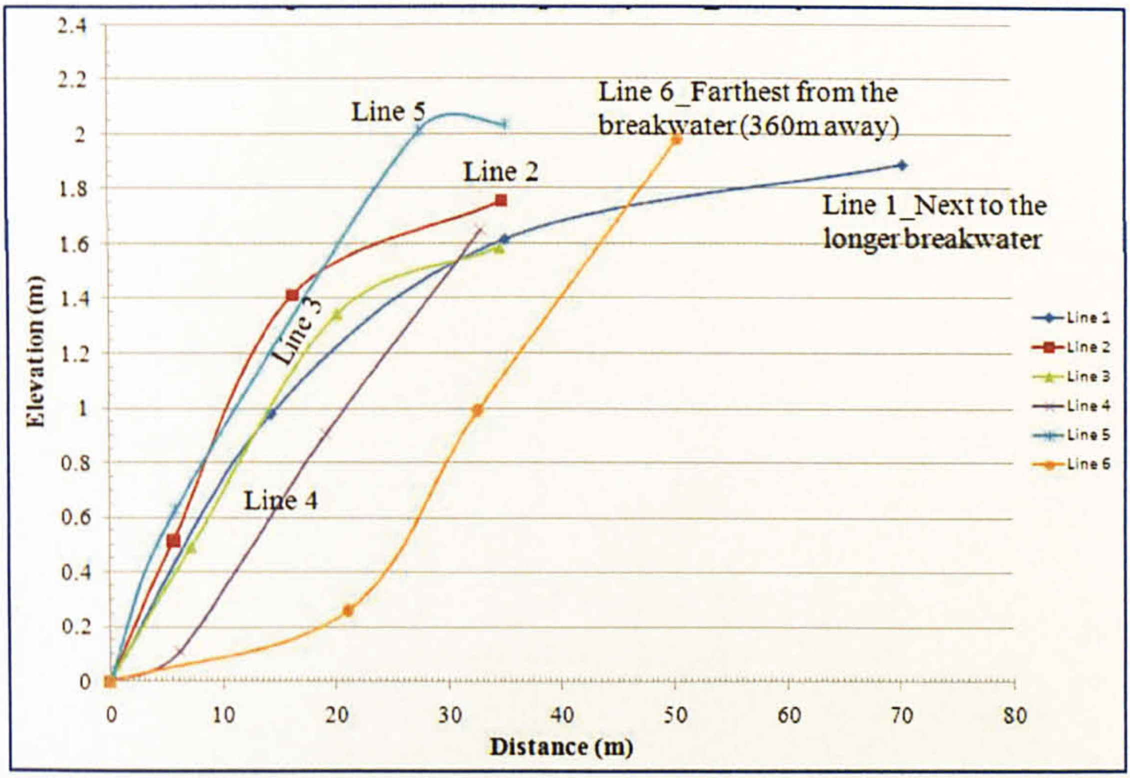

Figure A6.7: Slope of the beach along survey lines